# Theoretical studies involving two Diels-Alder reactions under solvent-free conditions

**Jonathan P. Miller ***

**Abstract**

Theoretical computational chemistry calculations involving two example cycloaddition reactions at the same temperature under solvent-free conditions have been carried out using a variety of computational chemistry methods including semi-empirical, *Ab initio* and DFT functional to estimate and determine their transition states (TS). The cycloaddition reactions involved the use of acrolein and 1-methoxybutadiene or thiophene and maleic anhydride as starting materials. The former lead to an asynchronous TS and the latter, synchronous. For the acyclic reactants, s-*cis* acrolein was found to be kinetically favoured, leading to the predicted *endo*-TS involving a polar Diels-Alder reaction. For the cyclic reactants, the *exo* was kinetically preferred, presumed steric in origin. Using an ELF topological analysis and also focusing on the Laplacian of the electron density, the nature of the TS was found to be non-concerted (stepwise) for 1-methoxybutadiene reaction, whereas in two stages for the cyclic reactants and this can also be seen along the IRC as bond formation occurs at different stages in the former and concertedly (synchronously) in the latter. It is likely that pseudoradicals are involved prior to intermolecular C-C bond formation.

**Keywords**

quantum mechanics, Diels-Alder reaction, HOMO, LUMO, semi-empirical, *Ab initio*, Hartree-Fock, DFT, B3LYP, MP2, transition state, IRC, NBO, ELF, electron localisation function, pseudoradical, Laplacian, 1-methoxybutadiene, acrolein, thiophene, maleic anhydride

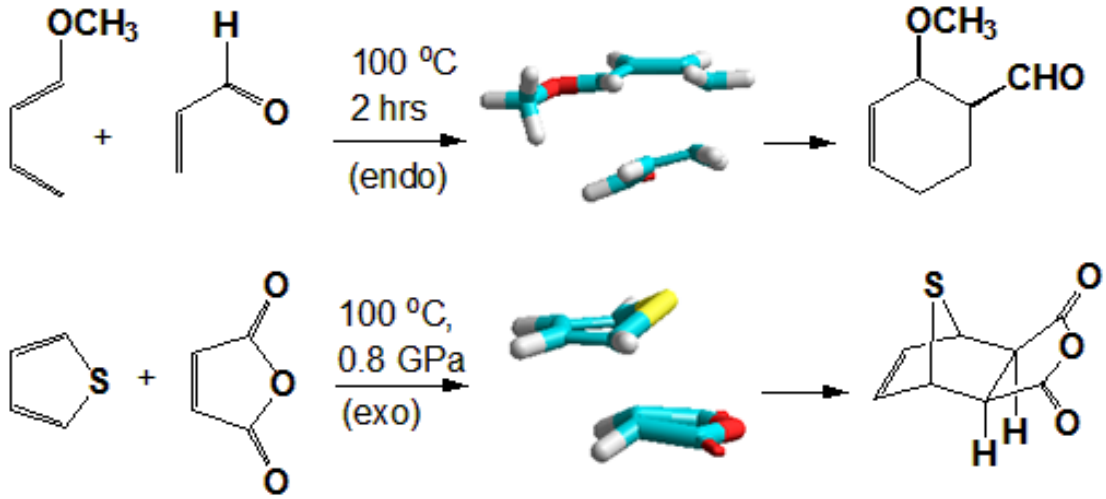


* jonathan.miller@alumni.manchester.ac.uk.

**1. Introduction**

The Diels-Alder reaction is a powerful synthetic tool in organic chemistry. Its versatility can provide up to four contiguous asymmetric centres with good yields, as many as three carbocyclic rings in the intramolecular and transannular variations, preference for *endo*-selectivity and facile manipulation of the cycloadducts. Its use is extended to dienes and dienophiles containing heteroatoms, aza-Diels-Alder and inverse-electron demand mechanisms [1-4].

Hückel perturbation MO calculations and the frontier molecular orbital (FMO) theory [5] obeying the Woodward-Hoffmann rules are traditionally used to predict regio-chemical and stereochemical outcomes in many reactions, including the Diels-Alder reactions. The majority of [4Πs + 2Πs] cycloadditions are concerted with aromatic transition states using this theory. Many decades ago, however, it was originally thought that the Diels-Alder reaction occurred by a diradical, non-concerted (stepwise) mechanism (prior to a frontier MO approach) [5].

Kohn-Sham density functional theory (DFT) [6-8] (and *Ab initio* Hartree-Fock (HF) [9]) methods allow a more accurate determination of HOMO and LUMO energies at a cost of computational time and hardware requirements compared to less expensive and quicker semi-empirical methods [10-12] (i.e. with far more approximations). The role of the Hamiltonian is different between two theories (i.e. DFT and HF) and DFT treats the electron correlation quite well. The development of DFT and modern quantum chemistry lead to the 1998 Nobel Prize in chemistry jointly awarded to W. Kohn and J. A. Pople [13].

More recently, on-going investigations [14] are still probing its mechanism (and also to test for concerted or stepwise [15] mechanisms). A study by Houk and co-workers in Los Angeles [16] found that at high temperatures the reaction of ethylene with butadiene occurred mostly by a concerted process (2% via a diradical process) using DFT (B3LYP 6-31G*) with the Gaussian 09 software package. Domingo and co-workers [17] have suggested that pseudodiradicals are involved with some non-polar Diels-Alder reactions (e.g. reaction of styrene with cyclopentadiene). Houk [18] also found that using DFT (with a more advanced functional method and basis set), the highly enantioselective organocatalytic Diels-Alder reaction of linear and cross-conjugated trienamines with oxindoles proceeded with a stepwise mechanism mainly via zwitterionic intermediates and not in the usual asynchronous concerted

manner as was previously thought. Deslongchamps [19] has qualitatively advocated that the regio- and stereochemical outcome of selected Diels-Alder reactions can be predicted via diradicaloids albeit with a concerted mechanism.

As a more illustrated example, a DFT study (B3YLP 6-31G* using Gaussian 03), including charge transfer and natural bond order analysis of the transition states, by Nacereddine and co-workers [20] found that the Diels-Alder reaction of methyl acrylate (or methyl methylacrylate, MMA) with furan in the absence of the $AlCl_3$ catalyst occurs via an asynchronous but concerted *endo*-transition state leading to the major stereoisomer. No *exo*-cycloadduct is observed experimentally using the MMA dienophile. In the presence of the catalyst, however, they were found to be non-concerted (stepwise). For the uncatalysed reaction, the bond lengths between the dienophile and diene differ by *ca.* 0.5 Å (2.400, 1.930 Å). Furthermore, Johnson [21] has applied the systematic electron transfer model (ETM) to many organic reactions (including the Diels-Alder reaction) using the DFT method (Spartan 10 and Gaussian 03 or 09 software) to optimise structures of the radical or radical ion intermediates. The Truhlar M05-2X functional and 6-31+G* basis set was utilised followed by vibrational frequency analysis. This model successfully reproduced observed regio- and stereoselectivities by analysis of spin density maps. This was in agreement with established frontier MO theory.

More recently, Domingo [22, 23] has suggested a new theory for the study of the reactivity in organic chemistry, called Molecular Electron Density Theory (MEDT) where the capability for changes in electron density (and NOT a MO approach) is responsible for molecular reactivity. The MEDT study involved conceptual DFT, ELF topological analyses (and associated energy changes) of the electron density for bonding changes along the reaction path (coordinate) and NCI of the transition states involved. ELF valence basins were also suitably described. For example, non-polar, polar and ionic Diels-Alder reactions were compared. MEDT thus provides a rationale for molecular mechanisms and reactivity.

Considering the current interest in theoretical aspects of the Diels-Alder mechanism, it was decided to probe two reactions, one leading to the *endo*-product (major) and the other only the *exo* in solvent-free conditions and to investigate whether computational (quantum)

chemistry could shed further light to the formation of one isomer (i.e. *endo*- or *exo*-product) and concertedness.

**2. Computational details**

All structures were geometrically optimised (equilibrium geometry) starting from the current geometry, for consistency, to provide a lower energy (local energy minimum on the PES) and a more stable structure. A conformer search can determine if it is indeed a global minimum. Chem3D Pro 5.5 (MOPAC 97) [24] provided the semi-empirical (PM3) geometry optimised structures (1-methoxybutadiene **1** and acrolein **2**) and HyperChem 8.0 [25] was used for further geometry optimisations where required. Using *Ab initio* with 1-methoxybutadiene **1**, the near-planar (s-*cis*) geometry changes to a near-gauche conformation. Spartan 14 [26] estimates a transition state from the product before the semi-empirical MNDO calculations were performed. Thiophene **7** and maleic anhydride **8** were geometry optimised starting from the MM+ geometry (HyperChem). All calculations were performed in gas phase (*in vacuum*) and unaltered thermodynamics. The quadratic Eigenvector Following Method (HyperChem) is sensitive to the starting geometries and spatial orientation of the reactants and they should be comparable for consistency. Initial starting geometries placed the dienophile and diene at *ca.* 1.95 ± 0.1 Å apart for the reacting atoms. Successful SCF convergence was reached when the RMS gradient got down to 0.01 kcal/mol/Ang or below. Firefly 8.2.0 [27] (partly based on US GAMESS version 6 [28]) was used for the DFT transition state searches (quadratic method), IRC calculations and NBO [29] analyses. For the TS and IRC calculations, the Hessian needs to be calculated from the initial geometry; vibrational calculations are also included by default (e.g. one imaginary frequency). The Hessian is known as the mathematical matrix of second derivatives of the energy with respect to geometrical coordinates.

QM software such as Chem3D, Spartan, HyperChem, Avogadro [30], Gabedit [31] and wxMacMolPlt [32] were used for generation or visualisation of the output structures (and orbitals) and wxMacMolPlt 7.7 for the IRC images. Avogadro 1.1.1 was used to prepare most of the input files for Firefly (without symmetry restraints); the default stationary point threshold

value of 0.0001 was used. Gabedit 2.4.8 was used for the Becke [33] and Savin [34] ELF topological analyses and Multiwfn [35] for the Laplacian of the electron density using a medium quality grid but using other default settings and the Becke ELF (usually high-quality grid setting = 0.06 Bohr and 0.3 size). The atom number labelling discussed in the text (e.g. C1-C2, C3-C4) are not associated with the labelling in the supplement. For HF and DFT, the popular 6-31G* basis set is seen as a good compromise between cost and accuracy; with these molecules larger basis sets were not necessary. The coloured phases of the molecular orbital surfaces obtained after the energy calculations are performed are arbitrary and can be swapped throughout the whole structure in the workspace. The bond orders between the molecules (C1-C2 and C3-C4) were obtained by examination of their properties after the calculations were complete. Some of this data is found in the supplement and in other files.

## 3. Results and Discussion

With the current global interest in determining energy data and transition states for named reactions including the Diels-Alder reaction, it was decided to estimate and determine transition states for several known Diels-Alder reactions with relatively small reactants. The current state-of-the-art focuses primarily on hybrid DFT (e.g. B3LYP 6-31G* or higher) or others such as the increasingly popular Truhlar M05-2X or post-Hartree-Fock MP2 correlation methods. *Ab initio* methods would provide a reasonable estimation of their corresponding transition states and energy data to begin to draw conclusive arguments for better accuracy with DFT. Some semi-empirical calculations were also undertaken for comparative purposes, which initiate the discussions.

### 3. 1 Transition State Analysis of the Reaction between 1-Methoxybuta-1,3-diene 1 and Acrolein 2

In the Diels-Alder reaction below, the reaction of 1-methoxybutadiene **1** (diene) with acrolein or propenal **2** (dienophile) gives exclusively the *ortho*-regioisomer in good yield [36], as a racemic mixture (compounds **3** and **4**). This reaction is regioselective (predominantly *ortho*-directing) and diastereospecific.

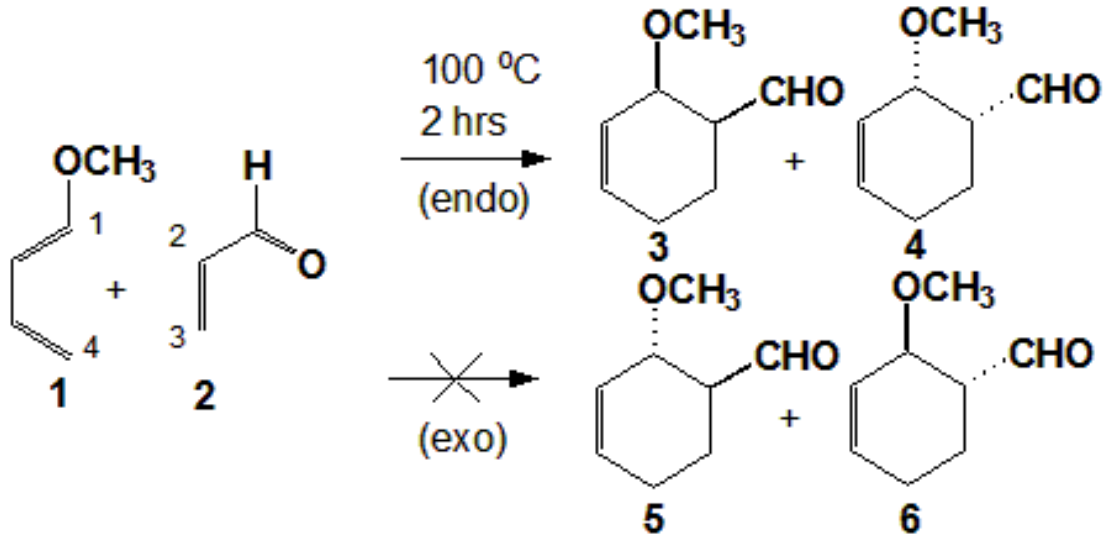


With achiral molecules, four stereoisomeric cycloadducts (**3-4** and **5-6**) are possible also depending upon whether the reaction is *endo*- or *exo*-selective.

**3.1.1 Semi-empirical (MNDO) Study**

The semi-empirical (MNDO) functional method was first used to estimate the transition state (TS1) for the reaction in the reaction scheme above. The asynchronous (*endo*) TS1 is shown below; it was estimated from a semi-empirical (MNDO) quantum-chemical (wavefunction) calculation/transition state optimisation technique with Spartan 14 with unaltered standard parameters *in vacuum* (thermodynamics:STP) and without using symmetry or other structural restraints anywhere during the process. The Hessian was found to have one negative Eigenvalue and energy (Heat of Formation) calculated to be 35.411 kJ/mol after 120 cycles. C1-C2 = 3.79 Å; C3-C4 = 1.78 Å. $E_A$ = 34.57 kcal/mol for reacting s-*cis* (31.0 kcal/mol for starting *s*-trans); reaction of ethylene and butadiene is 25.9 kcal/mol using the HF 3-21G [37] functional method. Mulliken Bond Orders are 0.091 and 0.535 and between C1-C2 and C3-C4. Natural charges are -0.304, +0.171, -0.046 and +0.093 for C3, C4, C1 and C2 (Mulliken charges the same). A semi-empirical (AM1) vibrational analysis with HyperChem 8 revealed that both *endo* and *exo*-products have the same energy (-67.06 a.u., 298.15 K) for their PM3 equilibrium geometries (Chem3D). The bond density image is also revealed, clearly showing the extent of the bond formation between C3-C4. Transition state geometries can vary depending upon the choice of functional method and/or basis set used [38] and the MNDO

data would appear to be an exaggerated likeness of the expected TS warranting further studies by *Ab initio* or DFT methods, as discussed below.

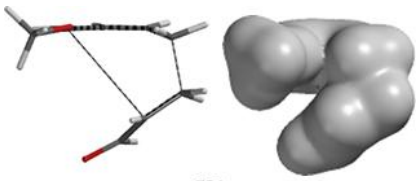

TS1

The asychronicity would appear to effect (i.e. reduce) the secondary orbital interaction (which is involved in reducing the energy of TS1) and the enantiomer **3** shown above results from this direction of approach. Reduction of secondary orbital overlap should indicate less preference for *endo*-selectivity (= *cis*-cycloadduct) from this extra stabilisation, but in the reaction, the *cis*-isomer is by far the major product (i.e. major diastereomer), as opposed to, say, a 70:30 or 50:50 cis/trans mixture of racemic cycloadducts. Preference of a *cis*-isomer instead of a *trans*-isomer is said to be kinetically preferred; the opposite, however, would be thermodynamic. This result is similar with other acroleins, such as ethyl acrylate [39].

The molecular orbitals are also displayed (in this case, leading to **3**); the HOMO for the diene **1** = -8.77 eV and LUMO for the dienophile **2** = -0.27 eV (or LUMO **1** = 0.38 and HOMO **2** = -10.73 eV). The energy gap ($E_{LUMO}$ - $E_{HOMO}$ = 8.50 eV or 820.1 kJ/mol) is in agreement with a previously reported value [40]. The global electrophilicity index, $\omega$, was calculated for dienophiles and dienes using the expression, $\omega = (\mu^2/2\eta)$ [41]. The electronic chemical potential $\mu$ and the chemical hardness $\eta$ were evaluated in terms of the FMO HOMO and LUMO, $\varepsilon$H and $\varepsilon$L, using the expressions, $\mu \approx (\varepsilon H + \varepsilon L)/2$ and $\eta \approx (\varepsilon L - \varepsilon H)$, respectively.

The global electrophilicity index, $\omega$, was calculated to be 0.96 and 1.45 eV for **1** and **2** respectively (compare this with reported [42] geometrically optimised values of 0.77 and 1.84 eV using DFT with the B3LYP functional method and 6-31G* basis set). The red and blue colours of the molecular orbital phases of the dienophile were swapped for the entire molecule after the calculation of their molecular orbitals; this is considered arbitrary. If the dienophile approaches from the alternative top face of the diene (with correct orbital overlap), this leads to the other enantiomer **4**. A chiral auxiliary or chiral catalyst is therefore required to

make this reaction stereoselective (enantioselective). Alternative views of the molecular orbitals of **1** and **2** are also displayed. The diene **1** has found early use [43] in constructing an achiral (racemic) tetracyclic anthracyclinone system (without ring-A functionalisation).

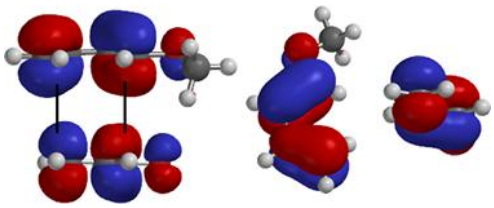

### 3.1.2 *Ab initio* Hartree-Fock Functional Methods

*Ab initio* methods generally allow for more accurate transition states to be determined (with less approximations) compared to semi-empirical methods. Hartree-Fock theory was developed to solve the electronic Schrödinger equation that results from the time-independent Schrödinger equation after invoking the Born-Oppenheimer approximation. The results are summarised in Table 1 for the extrapolated data. 1 Hartree (a.u.) = 2625.50 KJ/mol, 627.509 kcal/mol.

**Table 1.** Energy data/Hartrees (a.u.) for Transition States 2-10, intermolecular distances/Å, total dipole moment/Debye, vibrational analysis negative frequency/$cm^{-1}$ and LUMO-HOMO energies/eV for the dienophile and diene respectively.

| Entry | TS2 | TS3 | TS4 | TS5 | TS6 | TS7 | TS8 | TS9 | TS10 |
|---|---|---|---|---|---|---|---|---|---|
| **Energy** [a] | -456.953 | -456.954 | -459.499 | -459.501 | -456.8788 | -923.642 | -923.644 | -928.445 | -928.448 |
| **Energy** [a+] | -456.651 | -456.7146 | -459.062 | -459.263 | -456.1775 | -923.349 | -923.337 | -928.098 | -928.171 |
| **Energy** [b] | -456.739 | -456.741 | -459.287 | -459.289 | -456.668 | -923.495 | -923.497 | -928.297 | -928.301 |
| **Activation Energy** [b] | 25 | 25 | 34 | 35 | 76 | 34 | 35 | 49 | 51 |
| **C1-C2** | 2.41 | 2.56 | 2.60 | 2.72 | 2.91 | 2.17 | 2.15 | 2.16 | 2.19 |
| **C3-C4** | 2.06 | 1.98 | 1.97 | 1.94 | 1.73 | 2.17 | 2.15 | 2.16 | 2.14 |
| **$\mu^+$** | 5.9273 | 2.3917 | 5.9572 | 2.5112 | 7.4460 | 6.3244 | 4.9862 | 6.1163 | 4.6815 |
| **$\mu$** | 5.2340 | 2.1898 | 5.3278 | 3.1692 | 8.0454 | 7.0596 | 5.2209 | 6.8548 | 4.9418 |
| **Negative Frequency** | -696.27 | -656.99 | -738.65 | -717.41 | -635.97 | -705.86 | -719.23 | -747.94 | -763.17 |
| **LUMO** [c] | 2.49 | 2.49 | 2.41 | 2.41 | 2.62 | 0.69 | 0.69 | 1.05 | 1.05 |
| **HOMO** [d] | -7.98 | -7.98 | -7.92 | -7.92 | -8.51 | -9.10 | -9.10 | -8.94 | -8.94 |
| **$\Delta$E** | 10.47 | 10.47 | 10.33 | 10.33 | 11.13 | 9.79 | 9.79 | 9.99 | 9.99 |

[a] Obtained from the initial program output (absolute zero). [+]starting geometry prior to TS search (absolute zero). [b] After a vibrational frequency energy analysis (373.15K) for the TS (*Ab initio,* HyperChem). [c] LUMO of the dienophile. [d] HOMO of the diene using the same basis set as the TS search

For the starting geometry of acrolein **2**, the s-*trans* conformer is slightly thermodynamically preferred to the s-*cis* [44], although the use of s-*cis* is also reported [37] with other dienes. Another DFT study [45] found the TS from the s-*trans* conformer to be of slightly lower energy than the s-*cis*, although it also involved coordination to a cationic oxazaborolidine catalyst. It was therefore of interest to compare the energies, orbital interactions and geometries of the transition states for both conformers of acrolein. Although both s-*trans* and s-*cis* acrolein **2** furnished a TS with one negative Eigenvalue (and imaginary/negative frequency), the s-*cis* acrolein **2** provided a TS with very slightly lower energy/$E_A$. In addition,

both appeared similar in geometry and possess comparable MO surfaces. Much of data discussed below is for the latter.

A better representation of the asymmetric transition state is shown below, starting from the semi-empirical PM3 equilibrium geometry (Chem3D). After obtaining one negative Eigenvalue with HF 3-21G, TS2 (= *endo*) leads to the *cis* product, whereas the hypothetical TS3 (= *exo*) leads to the trans product, which is not observed in the laboratory. *Endo*-TS2 was found to be of slightly smaller negative energy than *exo*-TS3, suggesting minor involvement of secondary orbital stabilisation (to lower its $E_A$) for TS2 as mentioned above. The transition states were determined with HyperChem using a restricted *Ab Initio* Hartree-Fock (HF) 3-21G functional method, starting from geometrically optimised reactants (Chem3D semi-empirical PM3); relevant data is found in Table 1. For TS2 the bond orders = 1.17 and 1.21 respectively; for the hypothetical TS3 they are = 1.17 and 1.25. TS2 may be compared to the *endo*-TS starting from s-*trans* acrolein with bond distances of 2.44 and 2.05 Å (not shown). Related cycloadditions revealed C1-C2 and C3-C4 to be 2.73 and 1.94 Å for the reaction of s-*trans* acrolein with butadiene catalysed by $BH_3$ ($E_A$ = 17.52 kcal/mol) with the same basis set [46]. The $E_A$s are expected to be close to experimental. After the HF 3-31G geometry optimisation, the *endo*-cycloadduct **3** energy = -457.0621 a.u. (0 K) and *exo*-cycloadduct **5** energy = -457.0634, clearly quite similar. The Synchronous Transit (quadratic) Method was less rewarding resulting in the TS dienophile and diene becoming too close at *ca.* 1.5 Å using the s-*trans* acrolein **2** (not shown). A DFT B3LYP 6-31G* single-point energy calculation revealed for the PM3 geometry optimised **1**, the HOMO and LUMO = -5.244 and -0.371 eV and for **2** = -6.88 and -1.74 eV; the electrophilicity index, $\omega$, = 0.809 and 1.81 and eV respectively, similar to previously reported data [42]. This suggests that acrolein, **2**, would take part in a polar Diels-Alder reaction as $\omega \geq 1.5$. Sarotti [47] summarises the use of the electrophilicity index for Diels-Alder reactions in more detail. Analysis of the total dipole moments could not draw mechanistic conclusions (generally, they are lower in the TS than reactants).

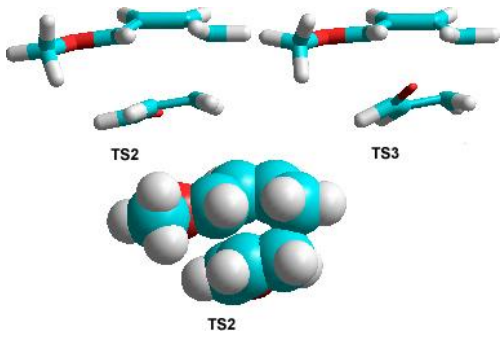


When the TS was calculated using the RHF 6-31G* method, to presumably determine a more accurate TS, a similar transition state (TS4) and scenario is observed; relevant data is found in Table 1. Bond orders = 1.36 (C1-C2), 1.27 (C3-C4) revealing the extent of the bond formation between C1-C2 and C3-C4, clearly better than in the semi-empirical studies, now suggesting an aromatic TS. The determined $E_A$s are overestimated, as can be expected with HF in general [48]. Interestingly, for *endo*-TS4, DFT RB3LYP-631G*//HF 6-31G* = 9.6 kcal/mol at 0 K, which could be considered less than experimental. Bond orders = 1.40 and 1.35 for *exo*-TS5. The HOMO (**4a**) and LUMO (**4b**) of the TS4 are also shown, confirming the extent of the bond formation between C1-C2; this scenario is similar in the *exo*-TS5 (not shown).

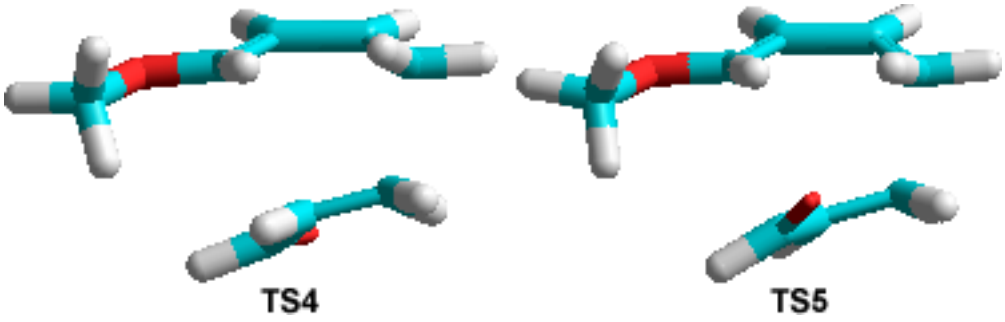


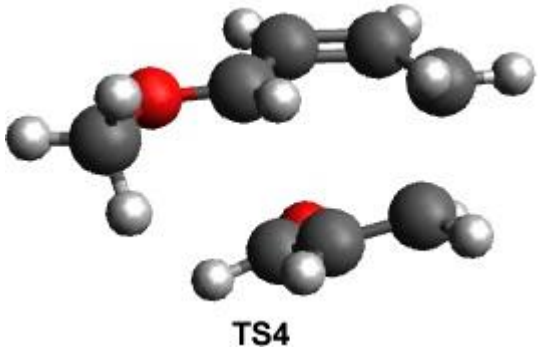

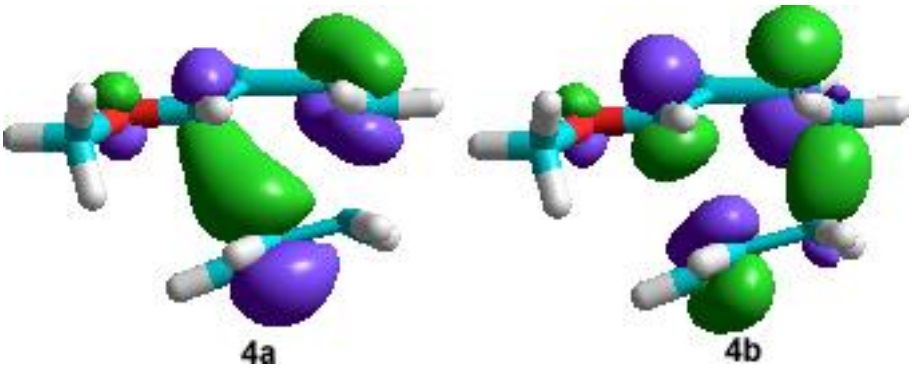


IRC calculations were then performed on the TS4 using Firefly. In the forward direction (product formation) one C-C bond is formed before the other suggesting a non-concerted (stepwise) mechanism. In the reverse drection, the IRC gives reactant-like character. The energy plot (see below: E along the PES reaction coordinate) and framed animation output (TS4_IRC.gif) from wxMacMolPlt is provided. Data from the Firefly NBO analysis is also provided (TS4_NBO.txt); using Firefly, the imaginary frequency is at -737.57 $cm^{-1}$ (TS4_FREQ.txt). Interestingly, using the Firefly output and then Gabedit to calculate the bond orders, they were found to be 0.223 and 0.512 for C1-C2 and C3-C4 respectively. The ELF topological analysis (isovalue 0.8) in blue clearly shows the start of the involvement of electron density for one C-C bond only, contradictory to any FMO bond order analysis!

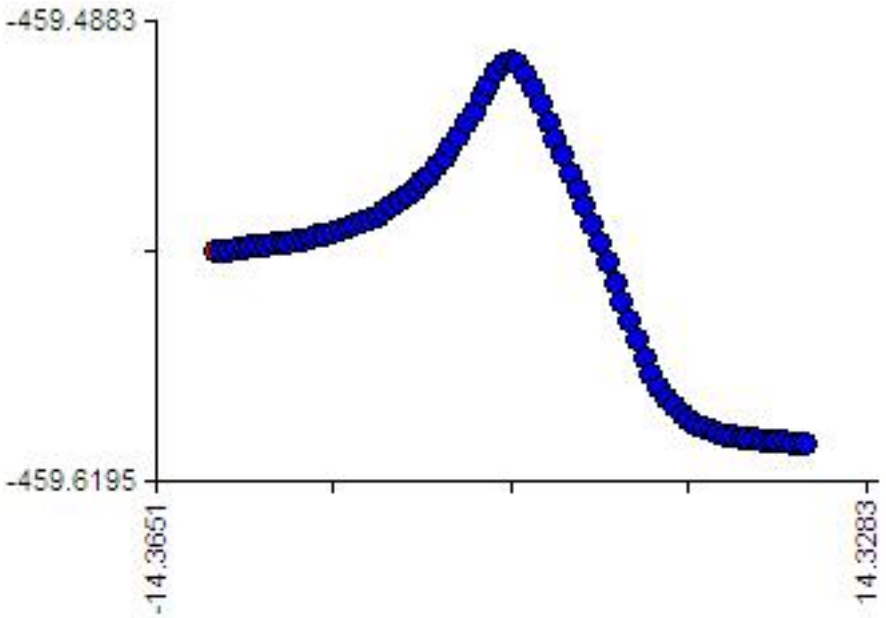

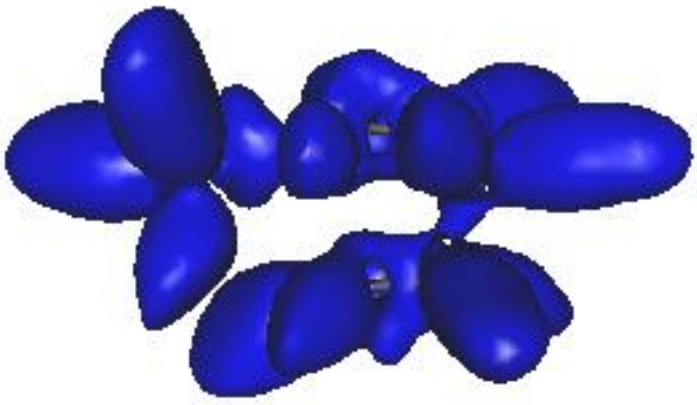

A Gabedit Savin ELF analysis with the same isovalue 0.8, the following is observed, indicating the absence of electron density formation between the molecules:

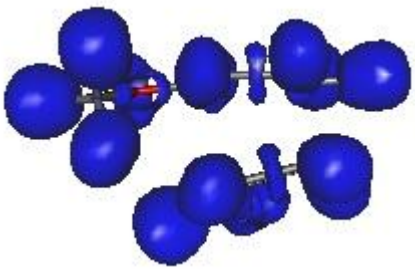

Using Multiwfn and two NBO output files (TS4.31 and TS4.40) focusing on its MOs (TS4.40), the Laplacian of the electron density (isovalue 0.8) the following is observed.

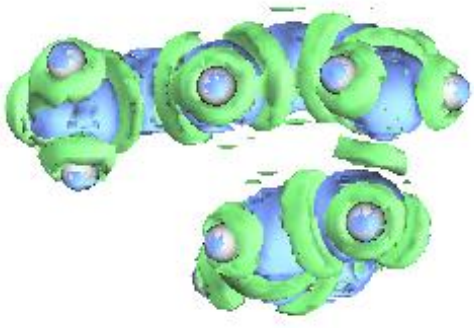

Using s-*cis* acrolein **2**, a successful TS search with the HF 3-21G* geometry optimised reactants has not been established. However using s-*trans* acrolein proved better (see also DFT studies below). The transition state (TS6) (RHF 3-21G*) reveals a different bond order determination (C3-C4 = 1.08 and C1-C2 = 0.005); The $E_A$ was overestimated at 76 kcal/mol

for the TS6 at 373.15 K, and similarly large using DFT RB3LYP 3-21G*//HF 3-21G* of 39.2 kcal/mol at 0 K. However, this time, a larger vibration 'between' C1-C2 is observed. Therefore, it is unlikely that the near-gauche form of 1-methoxybutadiene **1** is present in a more realistic TS as examination of the developing bonds/MOs are far from concerted and the $E_A$ much higher than the s-*cis* for this TS to develop under these conditions.

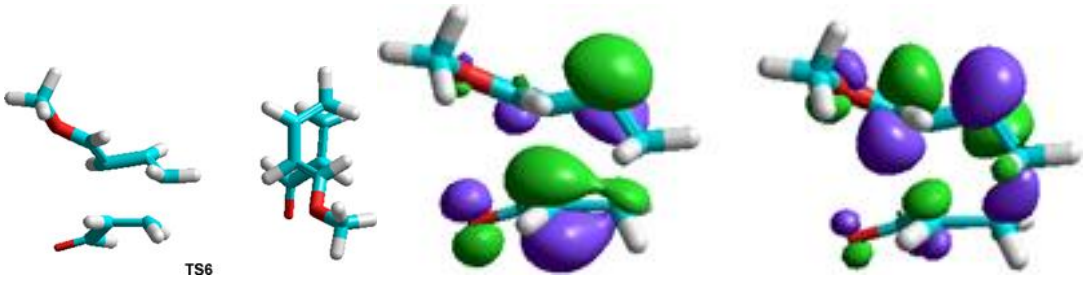


**3. 2 Transition State Analysis of the Reaction between Thiophene 7 and Maleic Anhydride 8**

Cycloaddition reactions of five-membered heterocycles such as thiophene **7** have been studied with a selection of dienophiles [49-52]. Planar thiophene **7** is found to be much less reactive than its carbocyclic counterpart due to its aromaticity involving the sulphur atom. Reaction of furan and and cyclopentadiene with maleic anhydride **8** [53, 54] affords the kinetically preferred *endo*-product due to the favoured secondary orbital overlap in its transition state and such observations would be expected with thiophene **7**, using a traditional FMO approach.

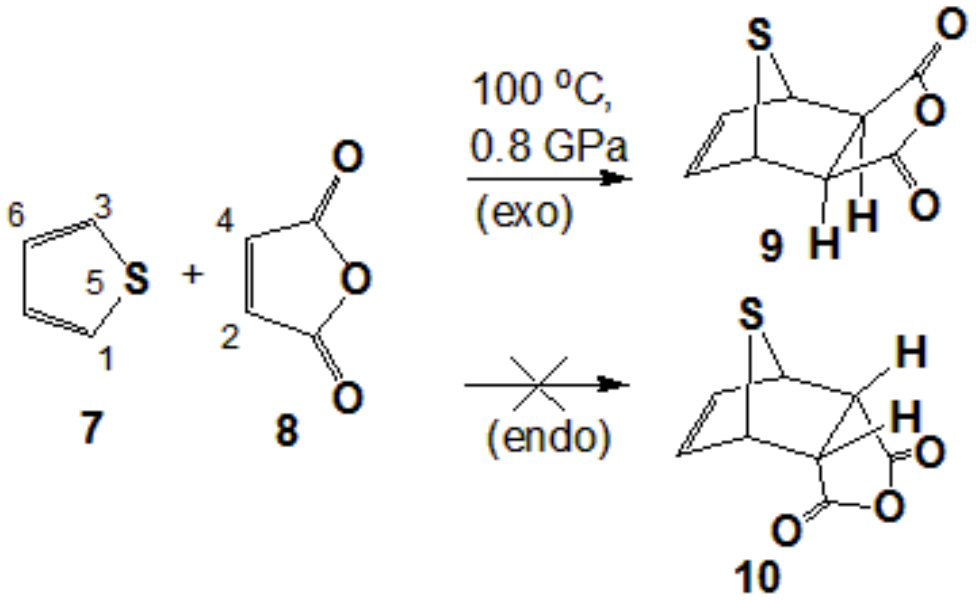


Some time ago [55], the reaction of thiophene **7** with maleic anhydride **8** in dichloromethane was found to occur at 15Kbar/100 $^{o}$C for 3 hours affording 37-47% pure *exo*-product **9**. More recently, the same reaction with maleic ahydride **8** occurs at the same elevated temperature and high pressure [56] under solvent-free conditions; in the scheme above only one mirror image of the racemate is shown. This reaction affords only the *exo*-cycloadduct (and absence of *endo*-cycloadduct **10**) and a theoretical investigation of its transition state has not been reported prompting further investigations in the present study. The computed energies of the geometrically optimised (HF 3-21G, 0 K) *exo*-cycloadduct **9** = -923.7206 a.u. and *endo*-cycloadduct **10** = -923.7191 a.u., considered similar in energy.

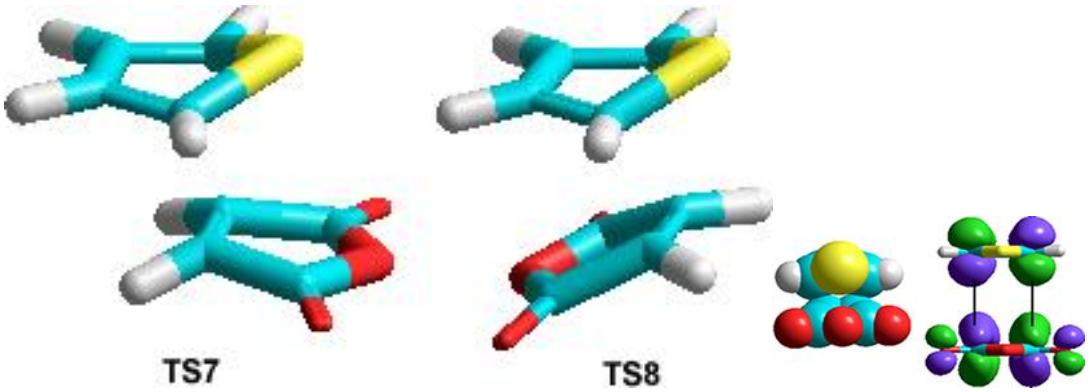


Starting from the HF 3-21G* equilibrium geometries , the semi-empirical (AM1) *exo*-transition state distances were found to be: C1-C2 = 4.83 Å; C3-C4 is = 4.75 Å, considered

unsatisfactory (as with the MNDO study above) due to the large intermolecular distances generated. It was therefore of interest to carry out a more accurate search for a TS with other functional methods. *Ab initio* methods were next chosen (HF 3-21G*). *Exo*-TS7 and *endo*-TS8 are shown above. Bond orders = 1.2 (TS7) and 0.3 (TS8) suggesting much more covalent bond formation between the molecules for the former. The $E_A$ are considered overestimated compared to any experimental. A similar result was observed with the Synchronous Transit (quadratic) Method to locate the TS (not shown). In order to try to obtain more accurate energy data, a larger basis set (HF 6-31G*) was chosen for the starting materials.

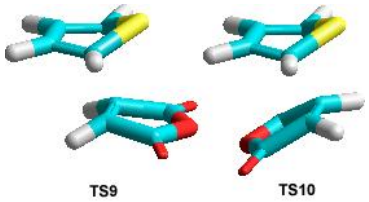


Similar to the smaller basis set, starting from planar thiophene **7**, a C1-S5-C3-C6 torsion angle for *exo*-TS9 = 30.97$^o$ and for *endo*-TS10 = 31.1$^o$. The bond orders between the bond forming atoms = 1.2 (TS9) and 0.2 (TS10), revealing product-like character. The $E_A$s were found to be overestimated, but better at 24 kcal/mol (semi-empirical AM1//HF 6-31G*) using energies obtained from a vibrational frequency analysis of the same TS. The IRC images correctly links the TS9 to reactant and product-like character (TS9_IRC.gif and TS9_IRC2.gif) and the energy plot is provided below; the program terminated early in the TS9 -> cycloadduct direction due to location very near a PES minimum (max. gradient = 0.000083; RMS gradient = 0.000030).

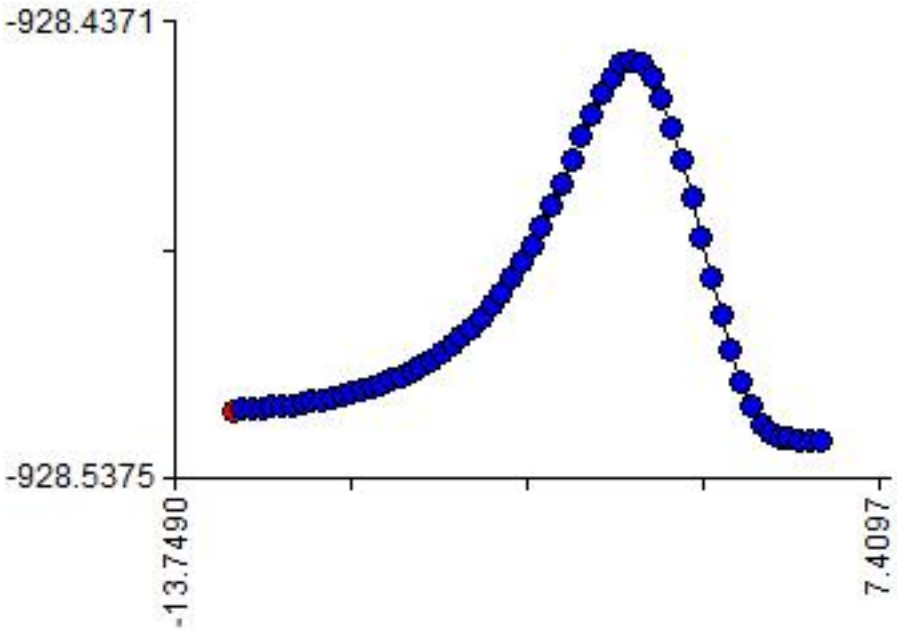


Data from an HF-6-31G* NBO analysis is also provided in an energy calculation of the TS (TS9_NBO.txt) and the frequency calculation reveals one imaginary frequency at -768.61 $cm^{-1}$. (TS9_FREQ.txt). The ELF topological analysis (isovalue 0.8) reveals electron density associated with the two developing C-C bonds.

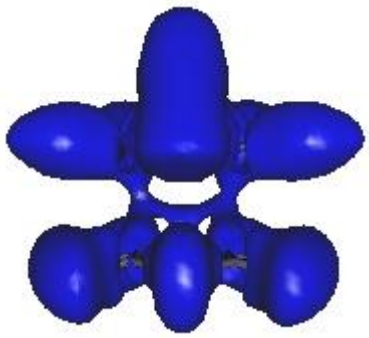

Using Multiwfn and two NBO output files (TS9.31 and TS9.40) focusing on its MOs (TS9.40), the Laplacian of the electron density (isovalue 0.8) is in agreement with the above.

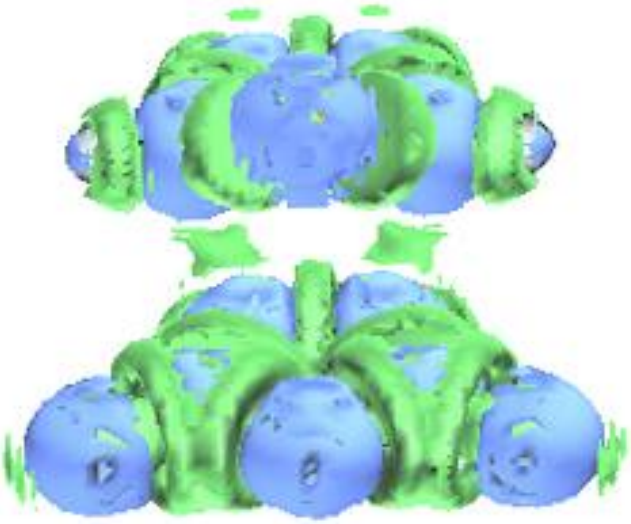

Considering the HF overestimated value, DFT B3LYP 6-31G*//HF 6-31G* (i.e. DFT energy on TS9 with HyperChem) furnished a more realistic value of 28.6 kcal/mol at 0 K. That the (unobserved) *endo*-TS10 has a slightly larger negative energy than the thermodynamically-preferred *exo*-TS9 (observed) suggests lack of involvement of any secondary orbital overlap or unfavourable FMO orbital interactions for the former and formation of one cycloadduct under these reaction conditions. Data from a DFT B3LYP 6-31G* NBO analysis is also provided in an energy calculation performed on the TS9 geometry (TS9_DFT.txt). In a specific ELF study using Multiwfn, the NBO file (DFT.37) revealed the following basin attractors (DFT_attractors.pdb); using HF 6-31G* NBOs are expected to be similar. The coloured image is Multiwfn visualisation output (0.1 Bohr) and the grey image is via Avogadro visualisation.

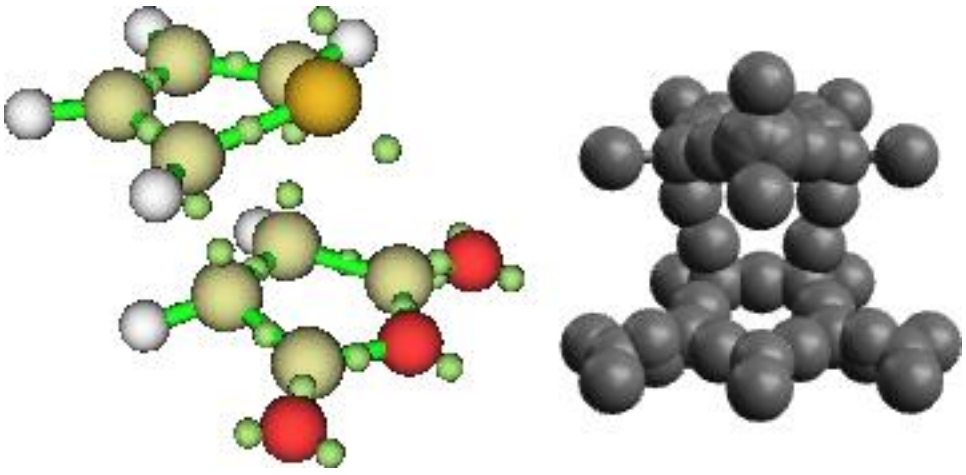

**4. DFT Transition State Studies with 1-methoxybutadiene 1 and acrolein 2**

The HF (6-31G*) TS suggests a good starting point for more accurate functionals with Firefly at the default 298.15 K (STP). Naturally, DFT is chosen to compare with the HF investigation. At that level of theory (RB3LYP 6-31G*) a similar TS is observed (TS11) with only one imaginary frequency (-409.07 $cm^{-1}$, TS11_FREQ.txt) and is fairly quick to locate the saddle point along the PES starting from the HF TS cartesian coordinates for input and generation of the required Hessian matrix prior to use with Firefly. The C1-C2 and C3-C4 bond lengths are 2.85 and 2.03 Å respectively; the bond orders were calculated to be 0.148 and 0.471 (Gabedit). It is similarly asynchronous to HF. Data from an NBO analysis is also provided in an energy calculation of the TS (TS11_NBO.txt). Using wxMacMolPlt, the C=C double bond is not seen in TS11!

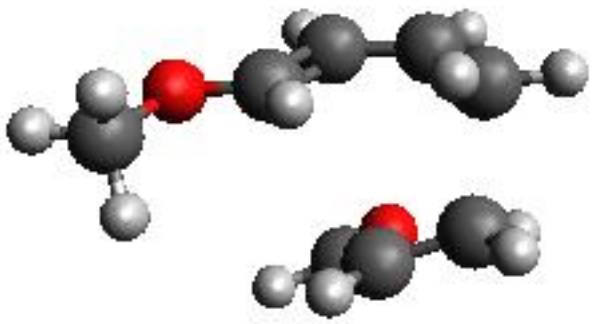

**TS11**

IRC calculations were then performed on the TS. In the forward direction (product formation) one C-C bond is formed before the other suggesting a non-concerted (stepwise) mechanism. Going along the IRC, the molecule markedly changes geometry -> product formation (cycloadduct). In the reverse drection, the IRC give the expected reactant-like character. The energy plot (see below with approx. bond forming regions) and framed animation output (TS11_IRC.gif, TS11_IRC2.gif and TS11_IRC3.gif) is provided. Similar to the earlier HF study, the ELF topological analysis (isovalue 0.8) in blue clearly shows the start of involvement of electron density for one C-C bond only, contradictory to any FMO approach.

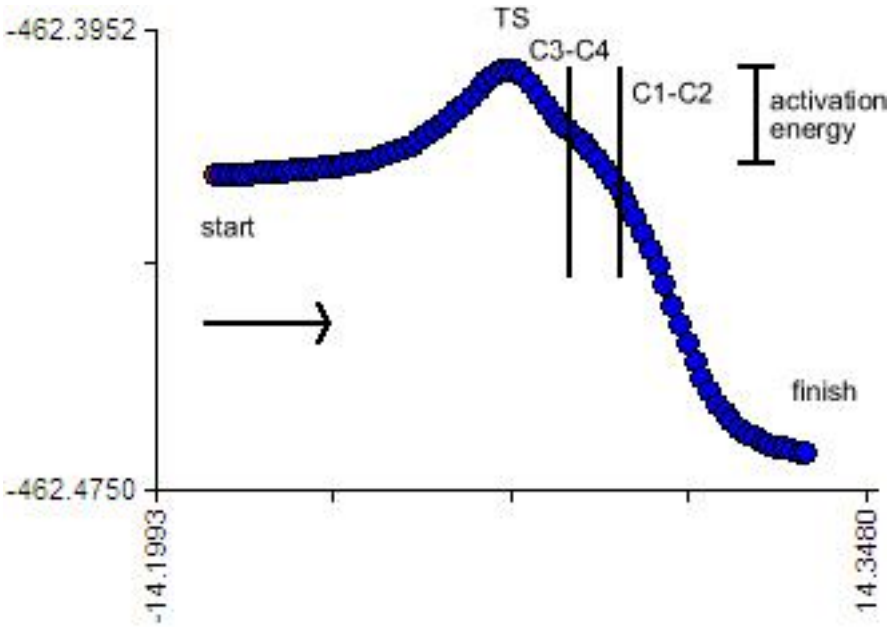


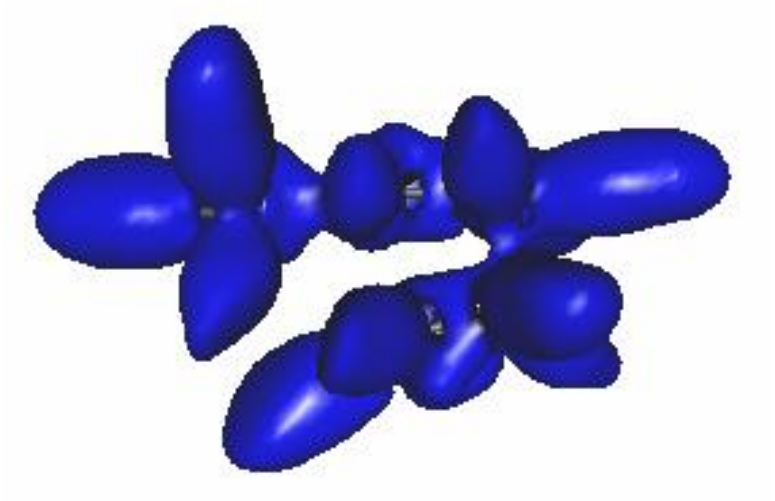

Using Multiwfn and two NBO output files (TS11.31 and TS11.40) focusing on its MOs (TS11.40), the Laplacian of the electron density (isovalue 0.8) is in agreement with the above.

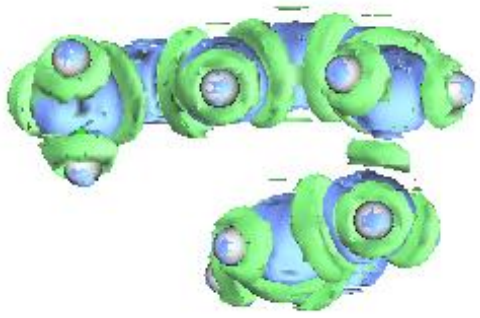

Using the NBO file (TS11.37), the following was produced by the Multiwfn ELF basin analysis showing the attractors (max. size 0.3) in the molecules and also available as TS11.pdf; note the absence of any attractors between the molecules (C---C) compared to TS9.

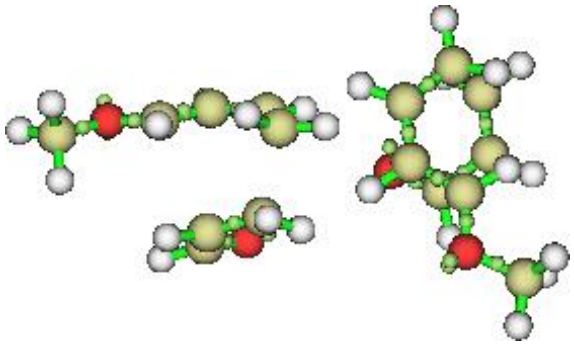

The critical points from midpoints of atom pairs (TS11.37) are revealed:

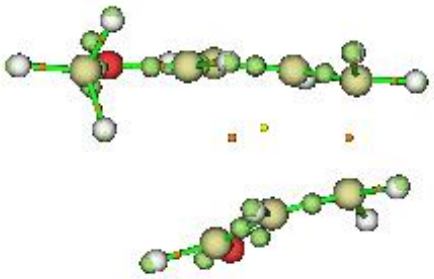

However, at point 7 after the TS (in the -> cycloadduct direction) along the IRC (TS11point7NBO.txt), using the NBO files (TS11point7.31 and TS11point7.37) the attractors are now seen for the C-3-C4 bond and before C1-C2 bond formation (output TS11point7.pdb); the attractors between the latter are likely to be due to the presence of 'pseudoradicals' (see also TS11_POINT7.txt and TS11_POINT7.jpg):

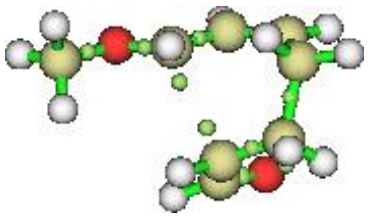

The Savin ELF (isovalue 0.8) is as expected for the new C-C bond:

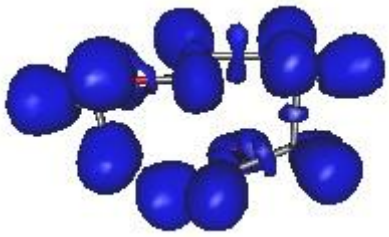

A virtually identical TS (TS11a) is observed (C1-C2 = 2.85 and C3-C4 = 2.03 Å) when starting with geometrically-optimised reactants (Firefly DFT B3LYP 6-31G*, reactants2.xyz) and $E_A$ = 10.81 kcal/mol with one imaginary freq. at 405.50 $cm^{-1}$ (TS11a_FREQ.txt). The IRC (TS11a.gif) is similar, with energy plot below and Gabedit ELF and Multiwfn ELF attractors via the NBO analysis (TS11a_NBO.txt using TS11a.31 and TS11a.37 plus TS11a.pdb output for the latter). Multiwfn ELF attractors (size 0.3) from the usual NBOs for path points 1-7 and 23-27 along the IRC after TS formation (-> cycloadduct direction) were combined in an animated GIF (ELFs.gif). This shows their involvement in new (asynchronous) bond formation. Output data is also provided (attract.txt) for the attractors and their identification numbering system changes going along the IRC geometries. The attractor values (not already part of an established bond) are <0.8 between C1 and C2 at path point 4 and <0.9 between C3 and C4 due to the start of involvement in the new covalent bond formation for the latter pair (a larger value). Their individual values for attractors 22,14, 12 and 16 (C1, C2, C3 and C4) = 0.764, 0.790, 0.834 and 0.858 on path point 4 (point4.jpg) as an example.

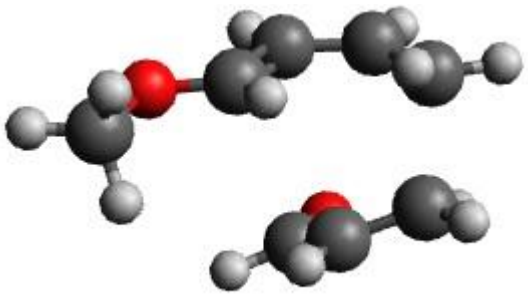

**TS11a**

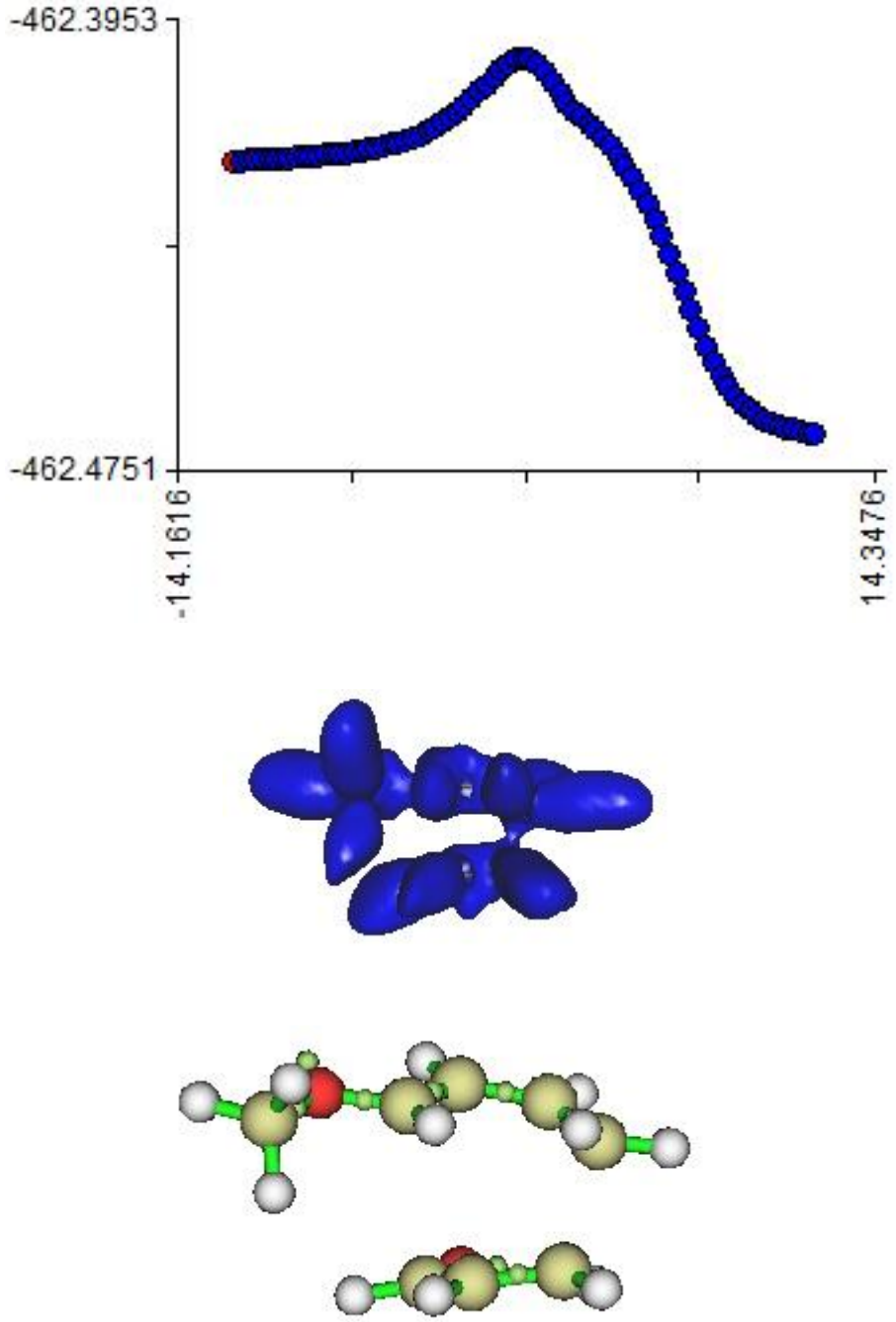


By way of comparison, when the Gabedit Becke isovalue is changed to 0.9, the following ELF analysis is seen:

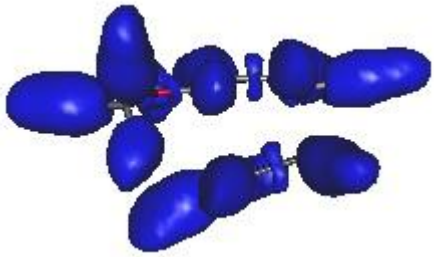

However, the Savin ELF analysis reveals a similar (or better) observation at isovalue 0.8:

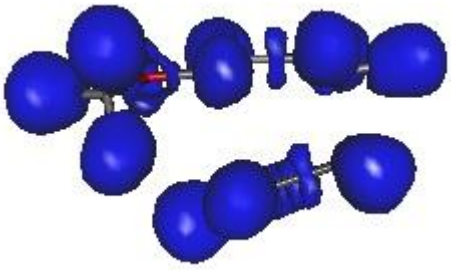

UB3LYP 6-31G* [17] was next chosen to investigate the likely pseudodiradical nature of the asynchronous TS11a, as it was found to better represent the attractors (UTS11a.37; UTS11a.31 not uploaded) and output UTS11a.pdb via NBO output (TS11a_UB3LYP.txt). Amongst others, the attractors on C2 and C4 are seen (TS11Ua.jpg). Analogous to above, the ELF attractors (size 0.3) from the usual NBOs for path points 41, 6 and 3 (TS -> reactants), TS and 4, 6, 22 and 41 (TS -> cycloadduct) were combined in an animated GIF (ELFs.gif). This shows their involvement in new (asynchronous) bond formation. Selected output data is also provided (UB3LYP.txt) for the attractors and their identification numbering system changes going along the IRC geometries.

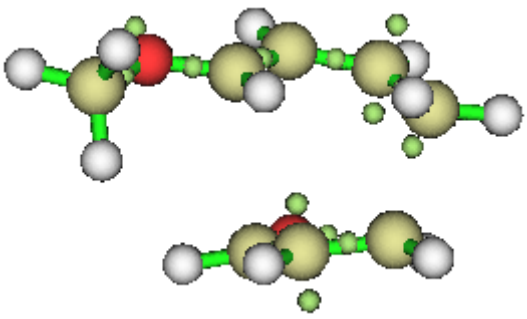

The final geometry from the IRC (-> cycloadduct direction) required geometry optimisation at the same level of theory to furnish the cycloadduct **3**. Energy data is provided (prod3.txt) and its energy is -462.4770 Hartrees. It appears to be a local minimum; a global minimum conformer search using Avogadro (MMFF94; Steepest Descent) caused a minor change in functional group geometry (**3a**).

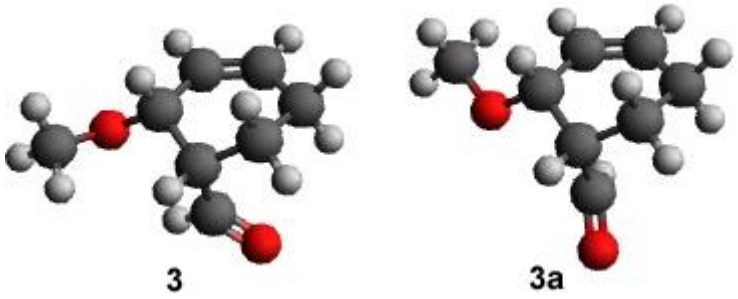


The proposed mechanistic pathway based on the IRC (and attractor ELF analysis) is shown below using the basic schematic geometries shown. The TS is seen near structure II with some of the 'pseudoradical' formation after the breaking of π-bonds. Going along the IRC, the bond between C3-C4 forms first (structure III), then as the geometry alters via structure IV (forming C=C double bond) to form the other C1-C2 bond for the cycloadduct (structure V).

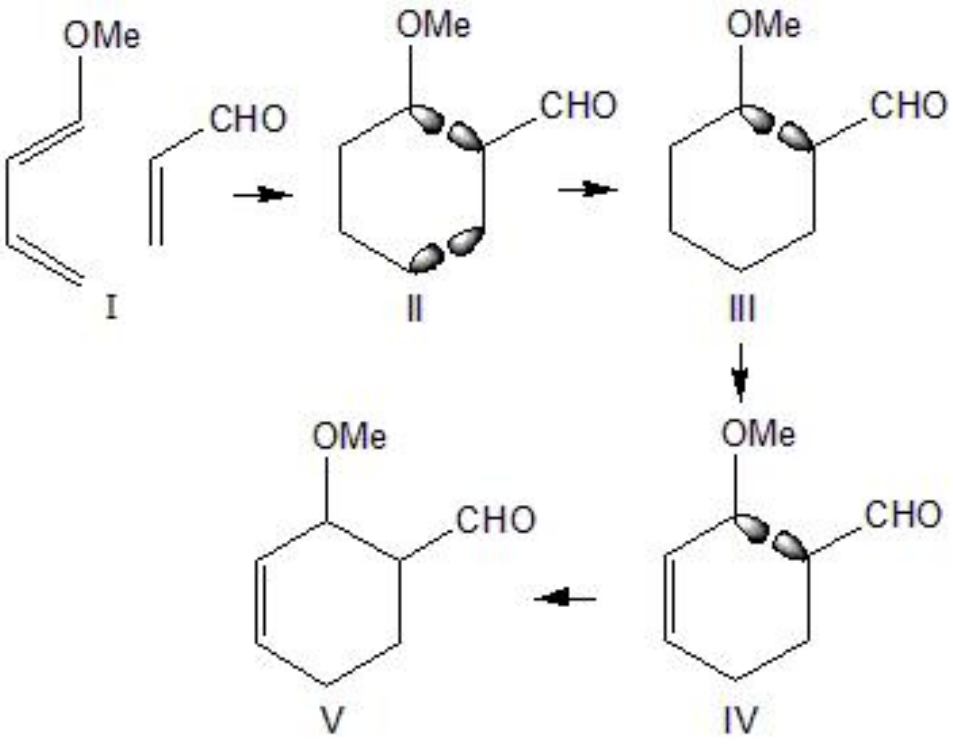

The geometrically optimised s-*cis* acrolein was subject to a conformer search with Avogadro and the s-*trans* acrolein is furnished. Subsequently it was used in a TS search replacing the s-*cis* acrolein from TS4. Using DFT B3LYP 6-31G*, TS12 was found as the stationary point on the PES with an imaginary frequency of -421.29 $cm^{-1}$ (TS12_FREQ.txt); $E_A$ = 10.5 kcal/mol (based on independent DFT geometrically optimised reactant energies). Going along the IRC (TS12_IRC.gif), the molecule markedly changes geometry -> product formation (cycloadduct). In the reverse direction, the IRC give the expected reactant-like character. The C1-C2 and C3-C4 bond lengths are 2.77 and 2.04 Å respectively; the bond orders for C1-C2 and C3-C4 were calculated to be 0.013 and 0.479 (Gabedit). Associated energy and NBO data are provided. Again, using wxMacMolPlt no C=C bond is seen in TS12.

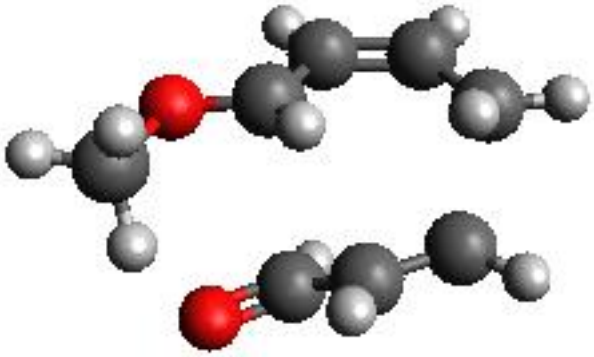

**TS12**

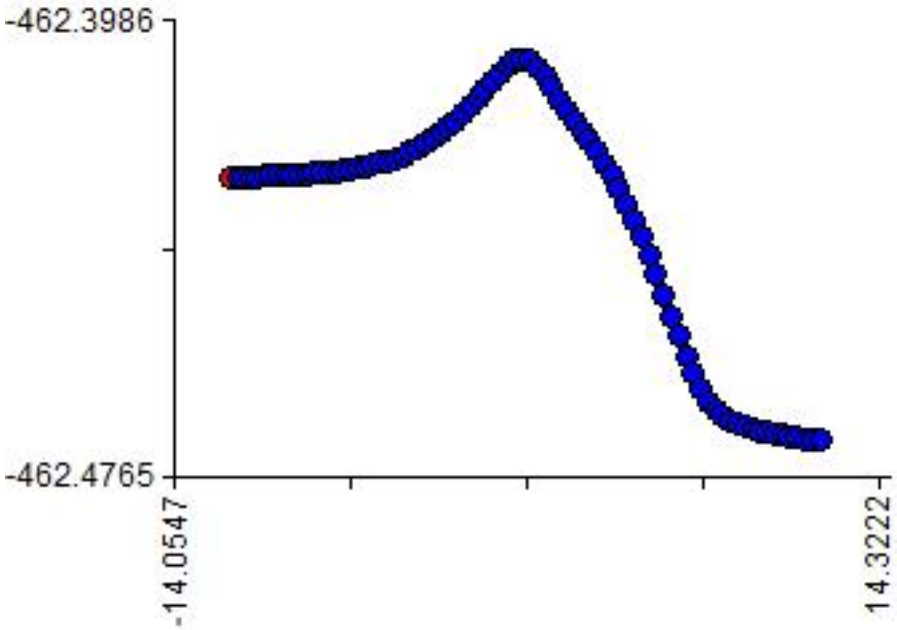

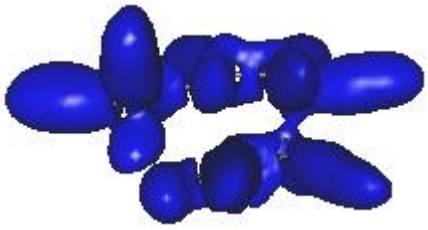

Using Multiwfn and two NBO output files (TS12.31 and TS12.40) focusing on its MOs (TS12.40), the Laplacian of the electron density (isovalue 0.8) is in agreement with the above and also similar to the s-*cis* conformer.

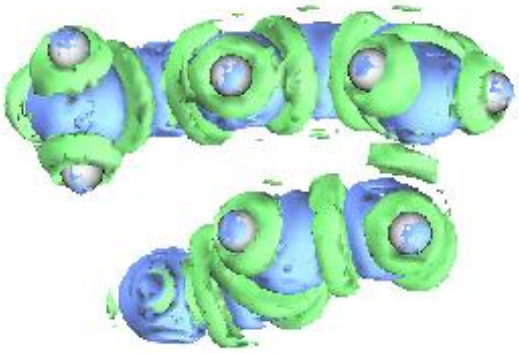

Similar to above, path point 7 on the IRC after TS formation (-> cycloadduct direction) gave the typical asynchronous bond formation and Multiwfn ELF attractors (output Trans7.pdb); it also suggests the presence of two 'pseudoradicals' between C1 and C2, prior to the new C-C bond formation:

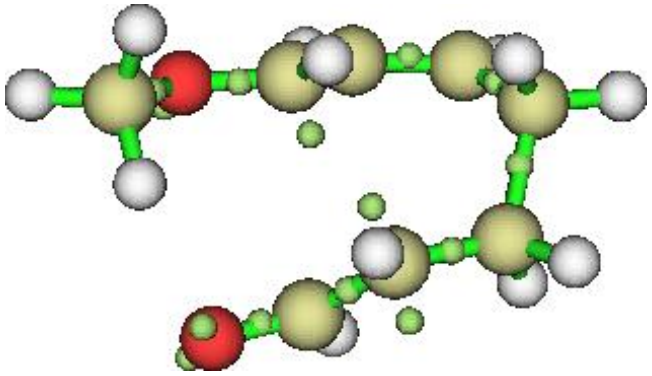

The final geometry from the IRC (-> cycloadduct direction) required geometry optimisation at the same level of theory  to furnish the cycloadduct **3b**. Energy data is provided (prod3b.txt)

and its energy is -462.4702 Hartrees. It appears to be a local minimum; a global minimum conformer search using Avogadro (MMFF94; Steepest Descent) caused a minor change in functional group geometry (**3c**).

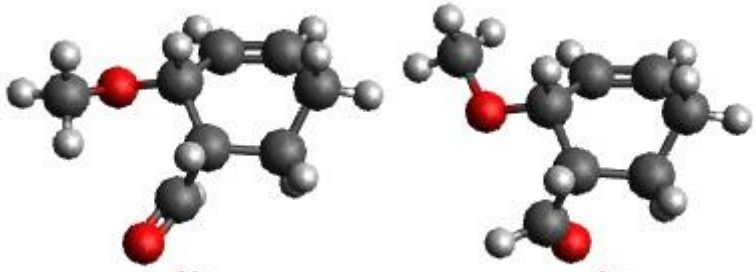


Strangely, using UB3LYP, no attractors were seen between the molecules (Utrans.txt & Utrans.pdb) for TS12 via the NBO output (UtransNBO.txt, Utrans.37; Utrans.31 not uploaded):

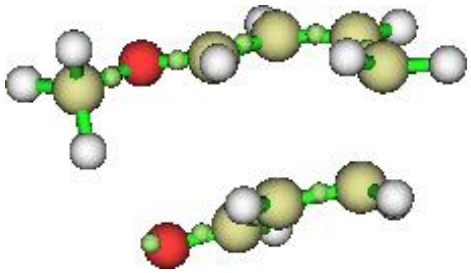

At a higher level of theory, DFT B3LYP 6-311G++(d,p), starting from the HF TS (and its calculated Hessian), a similar TS13 is observed with one imaginary frequency (-417.39 $cm^{-1}$ TS13_FREQ.txt) (+ early IRC -> to finish!): TS13.gif) and $E_A$ = 13.22 kcal/mol (using energies from independently determined reactants). The C1-C2 and C3-C4 bond lengths are 2.88 and 2.01 Å; the bond orders were calculated to be 0.276 and 0.377 (Gabedit). Energy and NBO data is provided (TS13_NBO.txt). The ELF topological analysis (isovalue 0.8) in blue shows the start of involvement of electron density for one C-C bond only, contradictory to any FMO approach. Once again, with wxMacMolPlt, the C=C bond isn't seen in TS13.

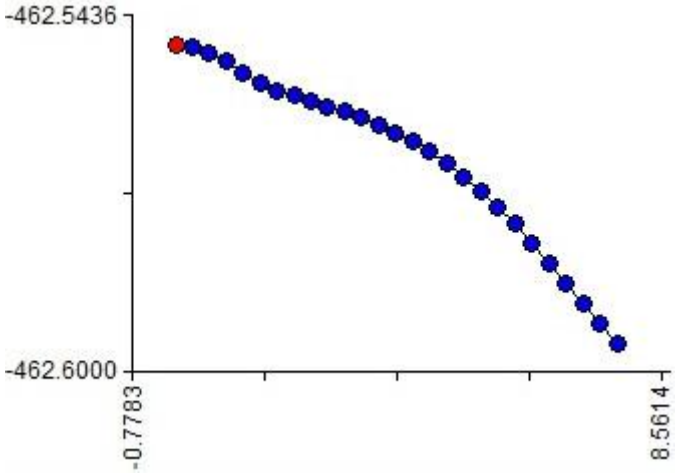


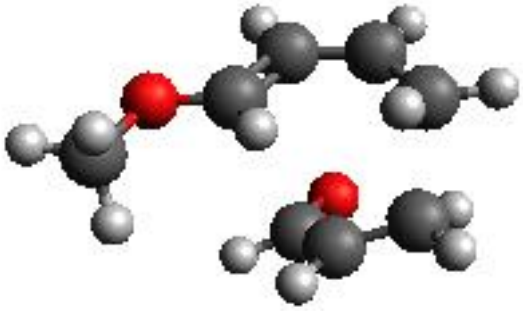

TS13

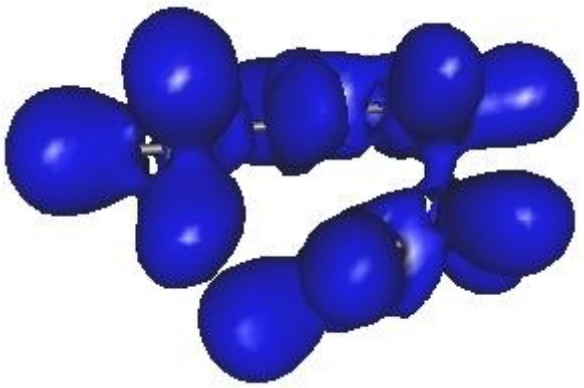

Using Multiwfn and two NBO output files (TS13.31 and TS13.40) focusing on its MOs (TS13.40), the Laplacian of the electron density (isovalue 0.8) is in agreement with the above.

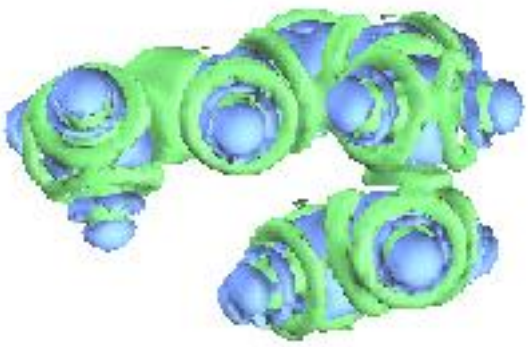

Once again, the Multiwfn ELF analysis using the TS13.37 NBO is similar to TS11 and output (TS13.pdb):

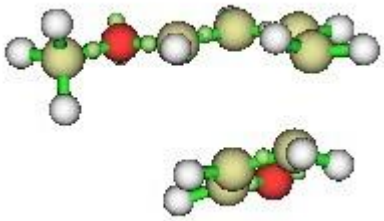

The final path point 29 along the IRC (TS -> cycloadduct) indicates that both covalent bonds have formed (Avogadro visualisation) as would be expected for this number of steps:

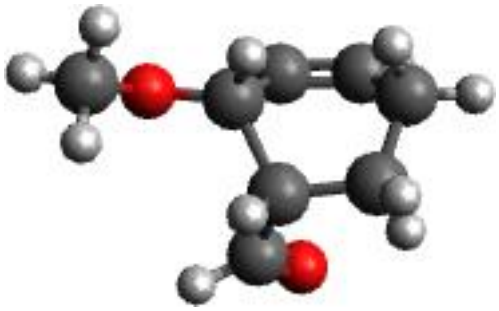

The UB3LYP ELF analysis reveals extra ELF attractors on the TS13 similar to the 6-31G* basis set; their output (adv_elf.txt , UB3LYPlab.jpg and adv_img.pdb) is provided via the their NBO files (TS13UB3LYP.txt and U13DFT.31 & U13DFT.37):

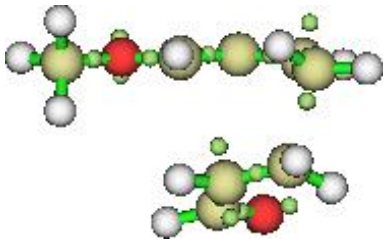

**5. DFT Transition State Studies with Thiophene 7 and Maleic Anhydride 8**

As with the acyclic Diels-Alder reaction, a DFT investigation was carried out starting from the previously determined HF 6-31G* TS9. Using the calculated Hessian (Firefly) for that TS, the DFT investigation furnished the TS13 considered similar in nature with one imaginary frequency (-534.22 $cm^{-1}$, TS14_FREQ.txt). The C1-C2 and C3-C4 bond lengths are 2.14 and 2.15 Å respectively; the bond orders were calculated to be 0.436 and 0.442 (Gabedit). $E_A$ = 29.0 kcal/mol. Associated energy and NBO data is provided (TS14_NBO.txt). IRC calculations (TS14_IRC.gif) and energy plot below were then performed on the TS14 using Firefly. In the forward direction (product formation), the C-C bond formations occur simultaneously. In the reverse direction, the IRC gives reactant-like character. The ELF topological analysis (isovalue 0.8) in blue clearly shows the start of involvement of electron density for two C-C bonds indicating an aromatic and concerted TS. This agrees with the FMO approach.

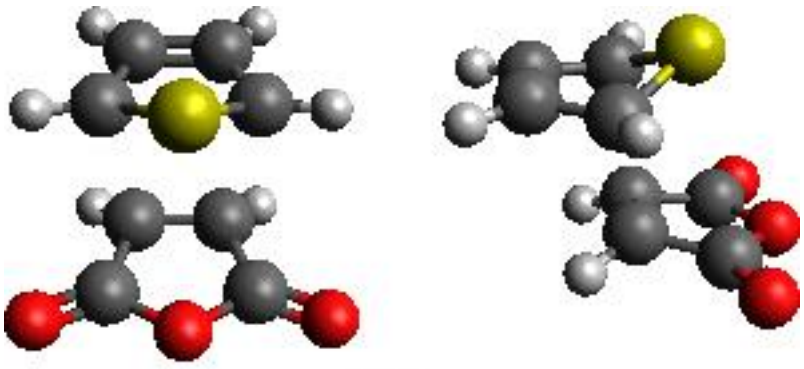

**TS14**

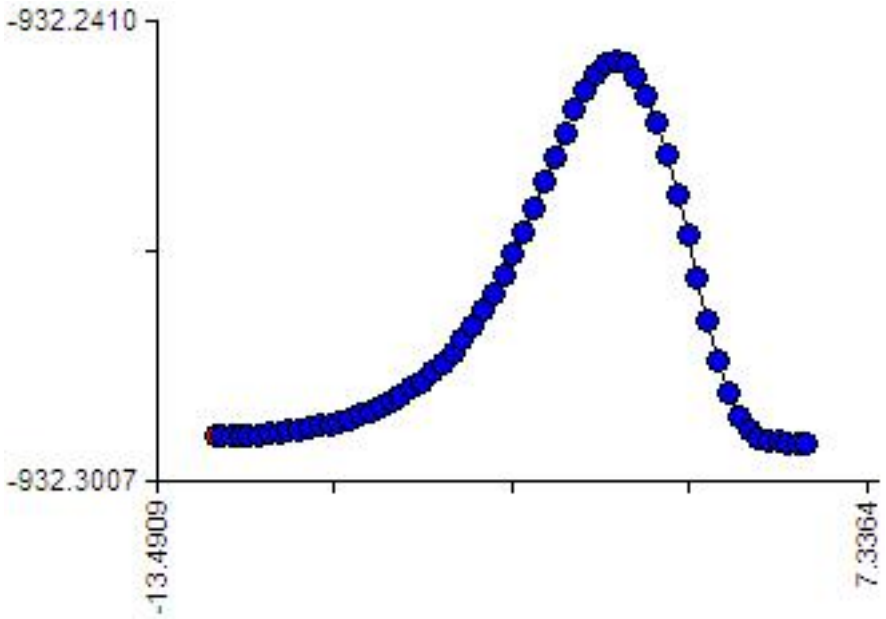


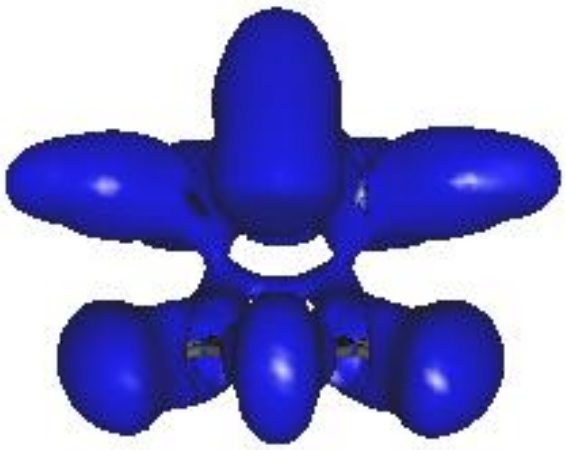

Using Multiwfn and two NBO output files (TS14.31 and TS14.40) focusing on its MOs (TS14.40), the Laplacian of the electron density (isovalue 0.8) is in agreement with the above, showing two C-C bonds forming.

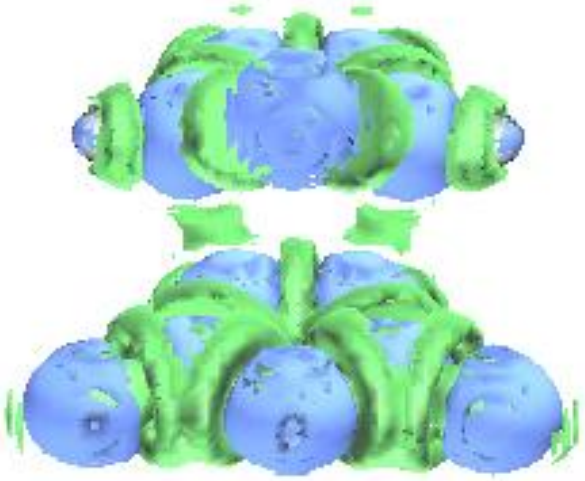

A virtually identical TS (TS14a) is observed (C1-C2 and C3-C4 = 2.15 Å) when starting with geometrically-optimised reactants (Firefly DFT B3LYP 6-31G*, reactants.xyz) and very close $E_A$ (29.03 kcal/mol) (imaginary freq. -537.08 $cm^{-1}$; TS14a_FREQ.txt). HOMO and LUMO **7** = -6.33 and -0.21 eV; HOMO and LUMO **8** = -8.14 and -3.19 eV; as expected, the HOMO **7** and LUMO **8** are closest in energy (3.14 eV). The global electrophilicity index, $\omega$ for **7** = 0.87 indicating it taking part in non-polar Diels-Alder reactions (for **8** it is 3.24 indicating it taking part in polar reactions). The IRC (TS14a.gif) is the same, with energy plot below.

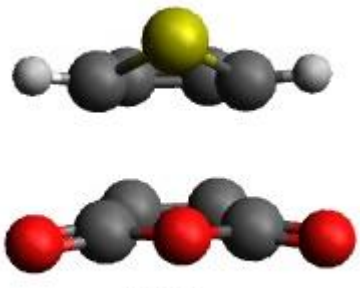

**TS14a**

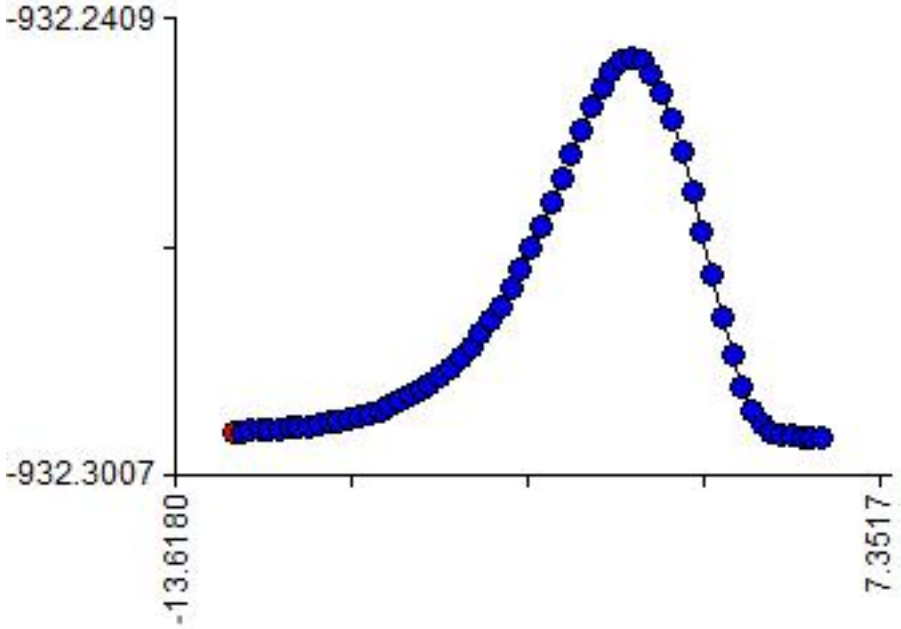


The Becke ELF analysis reveals the familiar intermolecular electron density arrangement:

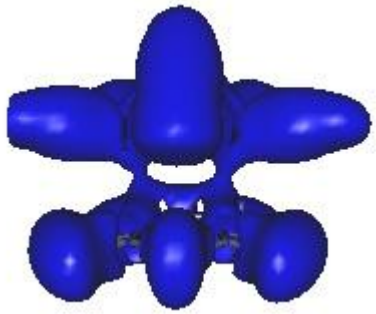

However, when the Becke isovalue of 0.9 is used, the following is observed:

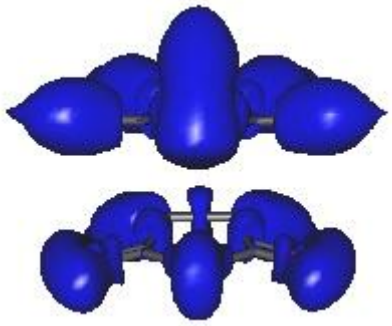

By way of comparison, the Savin ELF with isovalue 0.8 reveals a similar observation:

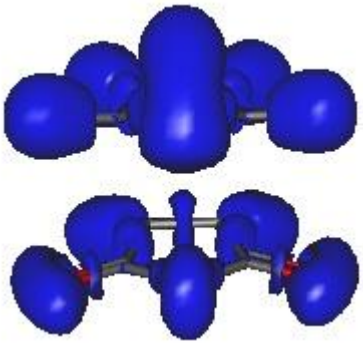

Again, the Multiwfn ELF basin analysis (0.06 Bohr) from NBO output (TS14a_NBO.txt and TS14a.31 and TS14.37) yields the same attractors between C1-C2 and C3-C4 and output is provided (TS14a.pdb).

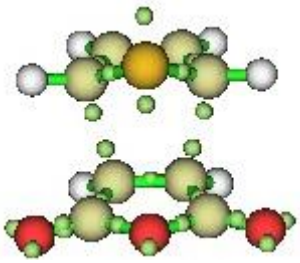

The final geometry from the IRC (-> cycloadduct direction) required geometry optimisation at the same level of theory to furnish the cycloadduct **9**. Energy data is provided (prod9.txt) and its energy is -932.2957 Hartrees. The final structure along the reaction coordinate (TS -> cycloadduct direction) was very close to the cycloadduct **9** as it only required two steps using geometry optimisation at the same level of theory to afford **9**.

**9**

Multiwfn ELF attractors (size 0.3) from the usual NBOs for path points (TS -> reactants) 5, 3, TS and path points (TS -> cycloadduct) 3, 6, 9, 10 and 11 along the IRC were combined in an animated GIF (THIO_ELFs.gif; size 0.3). Using as size of 0.2, the intermolecular attractors on path point 9 are separated. This shows their involvement in new bond formation after the TS, but the presence of 'pseudoradical' attractors before new intermolecular C-C bond formation. Output data is also provided (attract2.txt) for the attractors and their identification numbering system changes going along the IRC geometries. Attractors 29,27 and 30,28 for C1,C2 and C3,C4 respectively of TS14a show values of 0.799, 0.814, 0.801 and 0.815 (TS14a_ELF.jpg). Path point 10 (TS14a_ELF2.jpg attractors) seems to suggest one bond forming before the other which is unlikely for a symmetrical TS and now only one attractor between the atoms. Avogadro visualisation suggests both bonds have now formed; the basis analysis (basins **B27** and **B28**) is complementary.

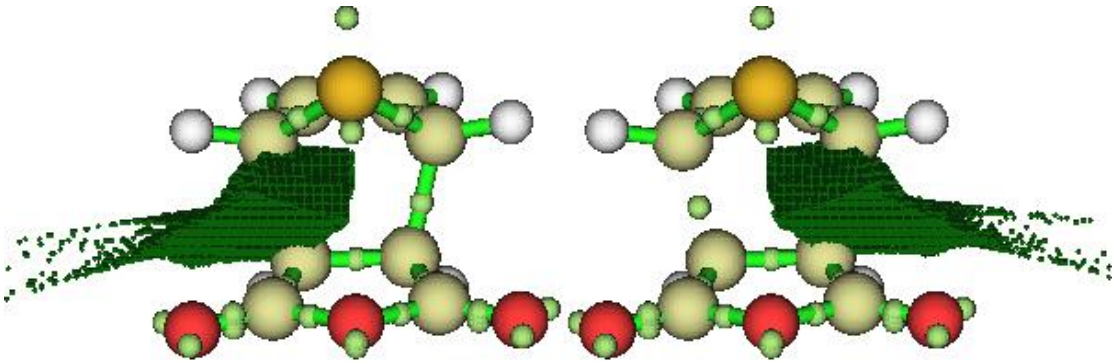


The UB3LYP ELF analysis reveals similar attractors on TS14 compared to the 6-31G* basis set; their output (ts14auelf.txt , Uts14alab.jpg and uts14a.pdb) is provided via the their NBO files (UTS14a.txt and U14aDFT.37; U14aDFT.31 not uploaded):

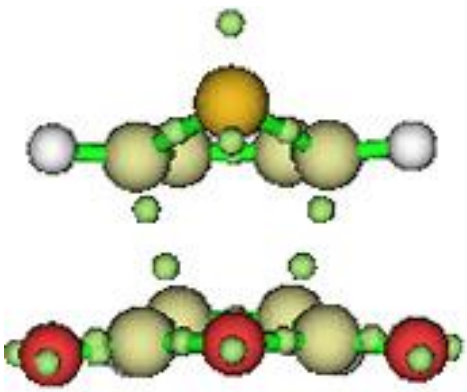

The scheme to show 'pseudoradicals' on the TS (H atoms omitted and geometry simplified) prior to C-C bond formation is presented. The amount of π-bond delocalisation and therefore any traditional aromatic character around the molecules is undetermined, which is normally the case for true concerted pericyclic reactions (using the FMO approach) with an aromatic TS. The presence of 'pseudoradicals' are likely to substantially reduce this and break π-bonds prior to pseudodiradical formation, but the new C-C bond formation is synchronous. This concept using ELF has been widely explored elsewhere using TopMod by Domingo [17].

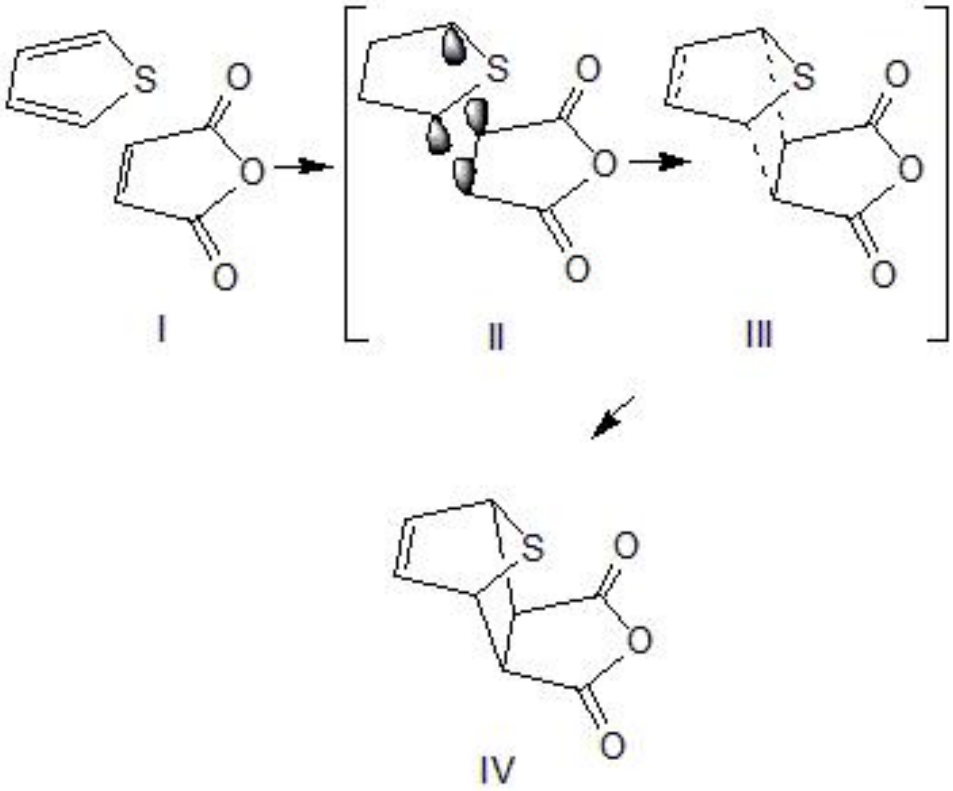


**6. MP2 investigation using 1-methoxybutadiene 1 and acrolein 2**

MP2 functional methods are an improvement on HF methods by adding electron correlation effects by way of the Rayleigh–Schrödinger perturbation theory [56]. An investigation at the MP2 level of theory using the 6-31G* basis set was carried out. Starting with the HF-631G* TS4 (and Hessian), TS15 was observed with one imaginary frequency (-399.99 $cm^{-1}$ TS15_FREQ.txt), $E_A$ = 5.29 kcal/mol mol (using energies from independently determined reactants) and again similar in nature to the *Ab initio* calculations. The TS15 -> cycloadduct energy curve along the IRC appears smoother than the DFT B3LYP version (TS11). The C1-

C2 and C3-C4 bond lengths are 2.63 and 2.16 Å respectively; the corresponding bond orders were calculated to be 0.129 and 0.304 (Gabedit). Associated energy and NBO data is provided (TS15_NBO.txt). The ELF topological analysis (isovalue 0.8) this time shows minimal electron density involvement for any C-C bond formation (partially contradictory to any FMO approach).

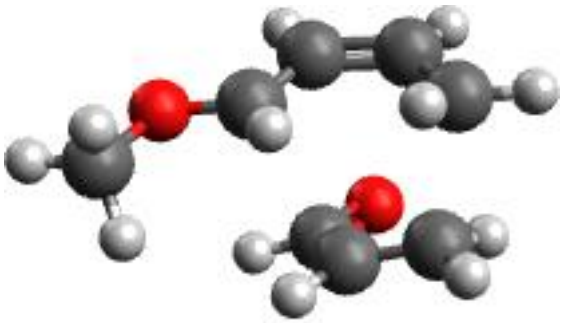

**TS15**

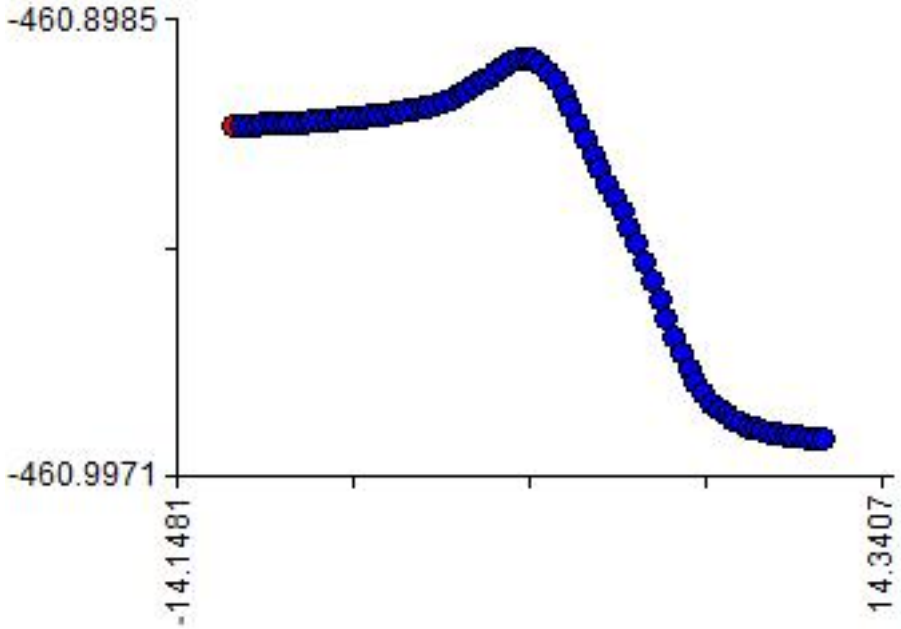

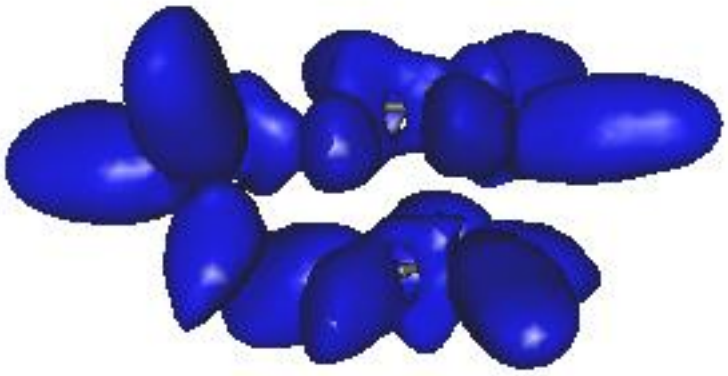

However, the electron density map (isovalue 0.05) in light blue shows the start of the C1-C2 covalent bond (Gabedit). Once again, with wxMacMolPlt, the C=C bond isn't seen in TS15.

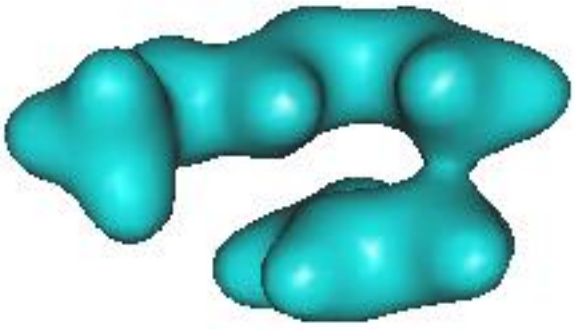

Using Multiwfn and two NBO output files (TS15.31 and TS15.40) focusing on its MOs (TS15.40), the Laplacian of the electron density (isovalue 0.8) is in agreement with the previous image.

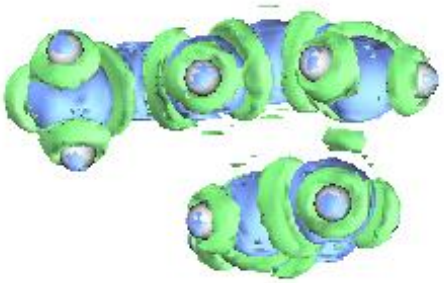

**8. Comparable Studies**

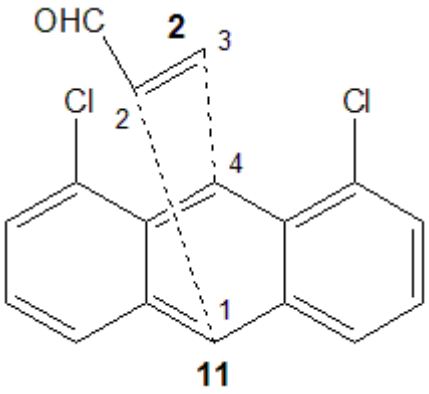


**11**

Recently, a DFT theoretical study of the Diels-Alder reaction reaction between 1,8-dichloroanthracene **11** and acrolein **2** (s-*cis* and s-*trans*) was explored [58] using the B3LYP functional and 6-311G(d,p) basis set. The *anti*-cycloadduct is the major isomer isolated in the laboratory (using $BF_3$ catalyst) by way of the approach above and with lower $E_A$. For their *TS-1*, the C1-C2 and C3-C4 distances were shown to be 2.59 and 1.99 Å. It was of interest to carry out a short ELF investigation on this, similar to the above, for comparative purposes.

Energy and NBO data is provided (TS16_NBO.txt) using the TS cartesian coordinates provided in the manuscript supplement [58]. The Becke ELF topological analysis (isovalue 0.8) in blue shows the start of involvement of electron density for one C-C bond only, contradictory to any FMO approach.

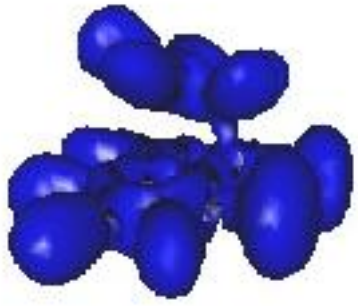

With the Savin ELF analysis (isovalue 0.5), there is a comparable observation:

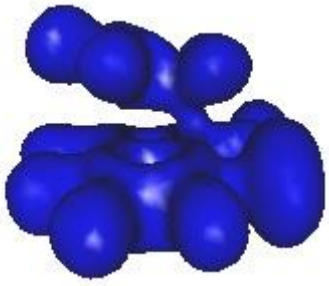

However, at isovalue 0.8 there is a noticeable difference and absence of intermolecular electron density (probably more realistic):

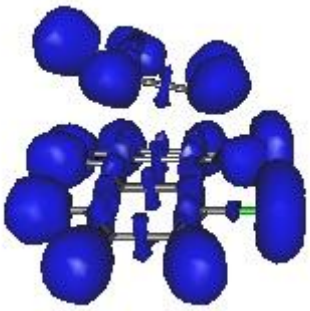

Using Multiwfn and two NBO output files (TS16.31 and TS16.40) focusing on its MOs (TS16.40), the Laplacian of the electron density (isovalue 0.8) is in agreement with the above.

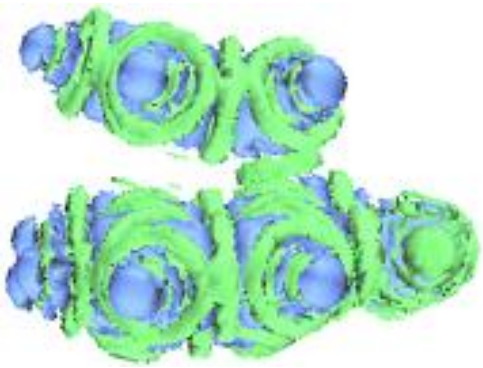

However, compared to the reaction between **1** and **2**, there are now some ELF attractors (0.06 Bohr) between the molecules (output anthr.pdb) - i.e. on the diene, suggesting the start of 'pseudoradical' formation.

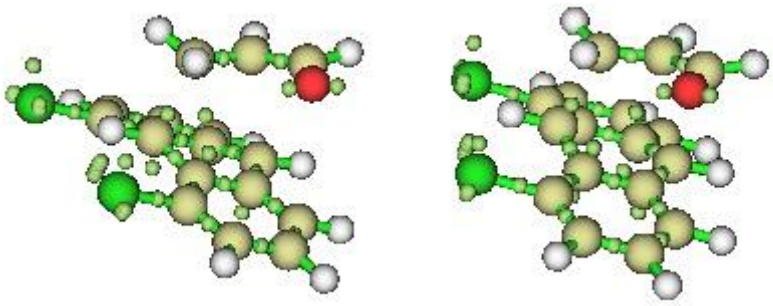

**7. Conclusions**

The present study has compared two Diels-Alder reactions that occur in solvent-free conditions at the same temperature using semi-empirical *Ab initio* and hybrid DFT functional methods; the latter two considered more accurate transition state representations to generate plausible qualitative arguments. The first reaction, involving acyclic starting materials (1-methoxybutadiene **1** and acrolein **2**) affords the *endo*-product. The second involving cyclic starting materials (thiophene **7** and maleic anhydride **8**) affords the *exo*-product. Its reaction also requires considerable pressure. In the former, the *endo*-TS is kinetically preferred and in the latter, it is the *exo* (the energies of the *endo*- or exo-TS for each reaction differ by only *ca.* 0.002-0.004 Hartrees at 373.15 K). This observation would suggest that the traditional secondary orbital overlap is not taking place with the geometries of the transition states obtained in the latter and likely to be thermodynamic/steric in origin. On the basis of TS searches and a basic ELF investigation, the reaction of the acyclic s-*cis* (or trans) dienophile and diene is expected to be non-concerted and stepwise with an asynchronous TS leading to the *endo*-product (contradictory to any FMO approach); the IRC showed the formation of the two intermolecular C-C bonds (i.e. TS -> cycloadduct) after the TS is reached and at different intervals. The s-*cis* and s-*trans* acrolein **2** were comparable (similar asynchronicity) in their transition states, albeit the s-*cis* being slightly lower in negative energy. It is likely that 'pseudoradicals' are formed prior to intermolecular C-C bond formation and best seen using UB3LYP.

For the cyclic dienophile and diene a synchronous TS leads to leads the *exo*-product, but it is also suggested that 'pseudoradicals' are formed prior to the synchronous (concerted) intermolecular C-C bond formation, the latter several steps after the TS on the reaction coordinate. The ELF and Laplacian of the investigation revealed the start of formation of electron density between the molecules; the Savin ELF requires a different isovalue for a similar observation. For both reactions, the HF geometry (6-31G*) was found to be a good starting point for further DFT (and MP2) studies and the TS from these was found to be similar in nature.

## References

[1] Cycloaddition Reactions in Organic Synthesis, S. Kobayashi, K.A. Jorgensen (Eds.,), Wiley-VCH Verlag GmbH, Weinheim, 2002.

[2] J.P. Miller, Recent Advances in Asymmetric Diels-Alder Reactions, in: J.C. Taylor (Ed.), Advances in Chemistry Research, Nova, New York, 2013, vol. 18, pp. 179-220.

[3] J.P. Miller, R.J. Stoodley, The use of D-glucose as a chiral auxiliary in asymmetric Diels-Alder reactions, J. Saudi Chem. Soc. 17 (2013) 29–42.

[4] R. Jasiński, Searching for zwitterionic intermediates in Hetero Diels-Alder reactions between methyl α,p-dinitrocinnamate and vinyl-alkyl ethers, Comput. Theor. Chem. 1046 (2014) 93-98.

[5] I. Fleming, Molecular Orbitals and Organic Chemical Reactions, Student edition, John Wiley and Sons, Chichester, 2009.

[6] W. Koch, M.C. Holthausen, A Chemist's Guide to Density Functional Theory, second ed., Wiley-VCH, Weinheim, 2001.

[7] S.M. Bachrach, Computational Organic Chemistry, John Wiley and Sons, Hoboken, 2014.

[8] A.J. Cohen, P. Mori-Sánchez, W. Yang, Challenges for Density Functional Theory, Chem. Rev. 112 (2012) 289-320.

[9] A. Hinchliffe, Molecular Modelling for Beginners (second ed.), Wiley, Chichester, 2008.

[10] M.J.S. Dewar, W. Thiel, Ground states of molecules. 38. The MNDO method. Approximations and parameters, J. Am. Chem. Soc. 99 (1977) 4899-4907.

[11] C. Cojocaru, A. Rotaru, V. Harabagiu, L. Sacarescu, Molecular structure and electronic properties of pyridylindolizine derivative containing phenyl and phenacyl groups: Comparison between semi-empirical calculations and experimental studies, J. Mol. Struct. 1034 (2013) 162-172.

[12] D. Margetić, R.N. Warrener, Ab initio and semiempirical modelling of stereoselectivities of Diels-Alder cycloadditions of furan and cyclopentadiene with norbornenes, Croat. Chem. Acta 76 (2003) 357-363.

[13] W. Kohn, Nobel Lecture: Electronic structure of matter—wave functions and density functionals, Rev. Mod. Phys. 71 (1999) 1253-1266.

[14] Y.-h. Lam, P.H.-Y. Cheong, J.M. Blasco Mata, S.J. Stanway, V. Gouverneur, K.N. Houk, Diels−Alder exo selectivity in terminal-substituted dienes and dienophiles: experimental discoveries and computational explanations, J. Am. Chem. Soc. 131 (2009) 1947–1957.

[15] S. Sakai, T. Okumura, Theoretical studies on the substituent effects for concerted and stepwise mechanisms of the Diels–Alder reaction between butadiene and ethylene, J. Mol. Struct. (TheoChem) 685 (2004) 89-95.

[16] K. Black, P. Liu, L. Xu, C. Doubleday, K.N. Houk, Dynamics, transition states, and timing of bond formation in Diels–Alder reactions, Proc. Natl. Acad. Sci. U.S.A. 109 (2012) 12860-12865.

[17] L.R. Domingo, E. Chamorro, P. Pérez, Understanding the mechanism of non-polar Diels–Alder reactions. A comparative ELF analysis of concerted and stepwise diradical mechanisms, Org. Biomol. Chem. 8 (2010) 5495-5504.

[18] A. Dieckmann, A. Breugst, K.N. Houk., Zwitterions and unobserved intermediates in organocatalytic Diels–Alder Reactions of linear and cross-conjugated trienamines, J. Am. Chem. Soc. 135 (2013) 3237-3242.

[19] G. Deslongshamps, P. Deslongchamps, Bent bonds and the antiperiplanar hypothesis as a simple model to predict Diels-Alder reactivity: retrospective or perspective? Tetrahedron 69 (2013) 6022-6033.

[20] S. Bouacha, A.K. Nacereddine, A. Djerourou, A theoretical study of the mechanism, stereoselectivity and Lewis acid catalyst on the Diels–Alder cycloaddition between furan and activated alkenes, Tetrahedron Lett. 54 (2013) 4030-4033.

[21] K.J. Cahill, R.P. Johnson, Beyond frontier molecular orbital theory: a systematic electron transfer model (ETM) for polar bimolecular organic reactions, J. Org. Chem. 78 (2013) 1864-1873.

[22] L.R. Domingo, Molecular electron density theory: a modern view of reactivity in organic chemistry, Molecules 21 (2016) 1319.

[23] L.R. Domingo, M. Ríos-Gutiérrez, P. Pérez, How does the global electron density transfer diminish activation energies in polar cycloaddition reactions? A Molecular Electron Density Theory study, Tetrahedron 73 (2017) 1718-1724.

[24] Chem3D Pro 5.5 CS MOPAC Std., CambridgeSoft, Cambridge, MA, 1999.

[25] HyperChem 8.0.10, HyperCube Inc., Gainsville, FL, 2009.

[26] Spartan '14, Version 1.0.0 Wavefunction, Inc. Irvine, CA, 2013.

[27] A.A. Granovsky, Firefly 8.2.0 http://classic.chem.msu.su/gran/firefly/index.html

[28] M.W. Schmidt, K.K. Baldridge, J.A. Boatz, S.T.Elbert, M.S. Gordon, J.H. Jensen, S.Koseki, N. Matsunga, K.A.Nguyen, S. Su, T.L. Windus, M.Dupuis, J.A. Montgomery, General atomic and molecular electronic structure system, J. Comput. Chem. 14 (1993) 1347-1363.

[29] E.D. Glendening, J.K. Badenhoop, A.E. Reed, J.E. Carpenter, J.A. Bohmann, C.M. Morales, F. Weinhold, NBO 5.9, http://www.chem.wisc.edu/~nbo5

[30] M.D. Hanwell, D.E. Curtis, D.C. Lonie, T. Vandermeersch, E. Zurek, G.R. Hutchison, Avogadro: an advanced chemical editor, visualization and analysis platform, J. Cheminformatics 4 (2012) 17.

[31] A.-R. Allouche, Gabedit-A graphical user interface for computational chemistry softwares, J. Comput. Chem. 32 (2011) 174-182.

[32] B.M. Bode, M.S. Gordon, Macmolplt: a graphical user interface for GAMESS, J. Mol. Graphics and Modelling 16 (1998) 133-138.

[33] A.D. Becke, K.E. Edgecombe, A simple measure of electron localization in atomic and molecular systems, J. Chem. Phys. 92 (1990) 5397-5403.

[34] A. Savin, B. Silvi, F. Colonna, Topological analysis of the electron localization function applied to delocalized bonds Can. J. Chem. 74 (1996) 1088-1096.

[35] T. Lu, F. Chen, Multiwfn: a multifunctional wavefunction analyzer, J. Comp. Chem. 33 (2012) 580-592.

[36] O. Wichterle, Sur les 1-alcoxy-butadiènes (1-oxyprènes), Coll. Czech. Chem. Comm. 10 (1938) 497-509.

[37] K.N. Houk, Ab initio and empirical computations of mechanism and stereoselectivity, Pure Appl. Chem. 61 (1989) 643-650.

[38] M. Linder, T. Brinck, On the method-dependence of transition state asynchronicity in Diels–Alder reactions, Phys. Chem. Chem. Phys. 15 (2013) 5108-5114.

[39] R. B. Grossman,The Art of Writing Reasonable Organic Reaction Mechanisms, second ed., Springer, New York, 2003, pp.183-195.

[40] Ref.[5] p. 227.

[41] R.G. Parr, L. Von Szentpaly, S. Liu, Electrophilicity Index, J. Am. Chem. Soc. 121 (1999) 1922−1924.

[42] L.R. Domingo, M.J. Aurell, P. Peréz, R. Contreras, Quantitative characterization of the local electrophilicity of organic molecules. Understanding the regioselectivity on Diels−Alder reactions, J. Phys. Chem. A 106 ( 2002) 6871-6875.

[43] F. Fariña and C.J. Vega, A novel route to tetracyclic hydroxyquinones. Tetrahedron Lett. 13 (1972) 1655-1658.

[44] G.-Y. Lee, H.-Y. Kim, I.-S. Han, DFT studies of the Diels-Alder reaction of 1,4-diaza-1,3-butadiene with acrolein, Bull. Korean. Chem. Soc. 20 (1999) 621-623.

[45] M.N. Paddon-Row, C.D. Anderson, K.N. Houk, Computational evaluation of enantioselective Diels-Alder reactions mediated by Corey's cationic oxazaborolidine catalysts, J. Org. Chem. 74 (2009) 861-868.

[46] K. A.Jorgensen, Theoretical Calculations of Metal Catalysed Cycloaddition Reactions, in: S. Kobayashi, K.A. Jorgensen (Eds.), Cycloaddition Reactions in Organic Synthesis, Wiley-VCH Verlag GmbH, Weinheim, p. 807, 2002.

[47] A.M. Sarotti, Unraveling polar Diels–Alder reactions with conceptual DFT analysis and the distortion/interaction model, Org. Biomol. Chem. 12 (2014) 187-199.

[48] M.K. Kesharwani, B. Ganguly, Solvent effects on the stereoselectivity of reaction of methyl acrylate,methyl methacrylate and methyl trans-crotonate with cyclopentadiene: A computational study, Croat. Chem. Acta 82 (2009) 291-298.

[49] T.H. Musslimani, H. Mettee, AM1 and PM3 semi-empirical study of the Diels–Alder reaction between N-, P-, O- and S-substituted aromatic heterocyclic five-membered rings with acrolein, J. Mol. Struct. (TheoChem) 672 (2004) 35–43.

[50] B.S. Jursic, Cycloaddition reactions involving heterocyclic compounds as synthons in the preparation of valuable organic compounds. An effective combination of a computational study and synthetic applications of heterocycle transformations, Comput. Theor. Chem. 5 (1998) 501-579.

[51] R. Vijaya, T.C. Dinadayalane, G. Narahari Sastry, Diels–Alder reactions between cyclic five-membered dienes and acetylene, J. Mol. Struct. (TheoChem) 589–590 (2002) 291–299.

[52] A. Ghomri, S.M. Mekelleche, Prediction of the chemo- and regioselectivity of Diels–Alder reactions of o-benzoquinone derivatives with thiophenes by means of DFT-based reactivity indices, Mol. Phys. 112 (2014) 566-574.

[53] L. Rulíšek, P. Šebek, Z. Havlas, R. Hrabal,.P. Čapek, A.Svatoš, An experimental and theoretical study of stereoselectivity of furan−maleic anhydride and furan−maleimide Diels−Alder reactions, J.Org. Chem. 70 (2005) 6295-6302.

[54] D.R.J. Palmer Integration of computational and preparative techniques to demonstrate physical organic chemistry concepts in synthetic organic chemistry: an example using Diels-Alder reactions, J. Chem. Educ. 81 (2004) 1633-1635.

[55] H. Kotsuki, H. Nishizawa, S. Kitagawa, M. Ochi, N. Yamasaki, K. Matsuoka, T. Tokoroyama, High pressure organic chemistry. III. Diels-Alder reaction of thiophene with maleic anhydride, Bull. Chem. Soc. Jpn. 52 (1979) 544-548.

[56] K. Kumamoto, I. Fukada, H. Kotsuki , Diels–Alder reaction of thiophene: dramatic effects of high-pressure/solvent-free conditions, Angew. Chem. Int. Ed. 43 (2004) 2015–2017.

[57] D. Cremer, Møller–Plesset perturbation theory: from small molecule methods to methods for thousands of atoms, WIREs Comput. Mol. Sci 1 (2011) 509–530.

[58] M.A. Sultan, U. Karama, A.I. Almansour, S.M. Soliman, Theoretical study on regioselectivity of the Diels-Alder reaction between 1,8-dichloroanthracene and acrolein, Molecules 21 (2016) 1277.

**Abbreviations**

DFT = Density Functional Theory

HF = Hartree-Fock

SCF = Self-Consistent Field

MNDO = Modified Neglect of Diatomic Overlap

AM1 = Austin Model 1

PM3 = Parameterized Model 3

B3LYP = Becke, 3-parameter, Lee-Yang-Parr

UB3LYP = Unrestricted Becke, 3-parameter, Lee-Yang-Parr

MP2 = Second Order Møller-Plesset Perturbation Method

TS = Transition State

IRC = Intrinsic Reaction Pathway

$E_A$ = Activation Energy

ELF = Electron Localisation Function

NBO = Natural Bond Order

PES = Potential Energy Surface

QM = Quantum Mechanics

FMO = Frontier Molecular Orbital

HOMO =Highest Occupied Molecular Orbital

LUMO = Lowest Unoccupied Molecular Orbital

6-31G* = 6-31G(d)